Inferring mode of locomotion through microscopic cortical bone analysis: A comparison of the third digits of *Homo sapiens* and *Ursus americanus* using Micro-CT

By

Kimberly D. Harrison

A Thesis submitted to the Faculty of Graduate Studies of

The University of Manitoba

in partial fulfilment of the requirements of the degree of

MASTER OF ARTS

Department of Anthropology

University of Manitoba

Winnipeg, MB

ABSTRACT

Bone is a 3D dynamic and unique tissue that structurally adapts in response to mechanical stimuli. Comparative skeletal morphology is commonly utilized to infer ancient hominins' modes of locomotion; however, instances of remarkable gross similarity despite different modes of locomotion do occur. A common cited example is the similarity between the skeletal elements of bipedal human (*Homo sapiens*) hands/feet and quadrupedal black bear (*Ursus americanus*) front/hind paws. Through novel 3D Micro-CT and 2D histomorphology analysis, this thesis tests the hypothesis that a 3D microscopic analysis of biomechanically regulated cortical bone structures provides a more representative and accurate means to infer a species' mode of locomotion. Micro-CT data were collected at the mid-diaphysis of human (n=5) and bear (n=5) third metacarpal/metatarsal pairs and compared with independent and paired t-tests, Pearson correlation coefficients and Bland-Altman plots. Bone microarchitecture is quantifiable in 3D and accessible through non-destructive Micro-CT. Interspecies variation was present, however no significant cortical differences between elements of humans and bears was found. Histological inspection revealed further variation both between and within species and element. A key limitation was sample size and further investigation of the relationship between mechanical loading and mode of locomotion is warranted.

ACKNOWLEDGEMENTS

I would like to first thank my advisor, Dr. Gregory G. Monks for your continual support and motivation, constructive feedback and uplifting words of encouragement which were most appreciated during the challenging portions of this research. I would also like to thank my committee members Drs. Robert Hoppa and David Cooper. Dr. Hoppa, thank you especially for helping acquire my samples which got this thesis off the ground. Dr. Cooper, thank you for providing your technical expertise and guidance throughout the thesis, it has been much appreciated!

Numerous individuals provided invaluable resources towards this thesis. Dr. Robert Hoppa and Mr. Stan Freer, thank you for providing access to the University of Manitoba's Department of Anthropology's teaching collection and Bioanthropology Digital Image Analysis Laboratory. Also, thank you to the University of Winnipeg's Department of Anthropology's Ms. Valerie McKinley, Dr. Barnett Richling and Dr. Michael MacKinnon for also providing me access to their teaching collections, equipment and laboratory. The bear paws utilized in this study, Manitoba Conservation (Permit # WB08992) was provided by Brandon University's Department of Archaeology's Biological lecturer Ms. Suyoko A. Tsukamoto, thanks again Suyoko! Thank you to the University of Saskatchewan's Department of Anatomy & Cell Biology's Dr. David Cooper for graciously provided me access to his laboratory, microcomputed tomography scanner and software. Finally, I would like to thank Dr. Theo Koulis and Mr. Richard Gagnon from the University of Manitoba's Statistical Advisory Service for providing their assistance with the statistical portion of this thesis.

Amy, Alex, Amanda, Emma, Rachel, Julia, Sarah, Dave, Kate, Marcelle, Stephanie, Lesley, Tim, Val, Cheryl, Isaac and Yasmin, thank you all for your sources of knowledge, motivation, technical expertise, but most importantly, the laughs and good times! I also want to extend my sincere thanks to Ms. Valerie McKinley. Val, your continuous support, encouragement and understanding for the last two years of my degree was a constant source of drive for me to complete this research and for that I'm always grateful. Last, but not least I would like to thank my family. Mom, Dad, Audra and Mike your ongoing interest and encouragement in my studies has been invaluable. Thank you for always supporting me and giving me advice when I needed it most

Finally, I would like to acknowledge the individuals and institutions that financially supported this thesis. Thank you to the University of Manitoba's Department of Anthropology for awarding me the Thesis-Direct-Related Costs Funding Scholarship. Also, thank you to the University of Manitoba's Faculty of Arts for awarding me the Graduate Thesis-Write-Up award. I would also like to thank the University of Winnipeg's Department of Anthropology's Dr. Barnett Richling for providing funds to aid in research costs and also to Ms. Valerie McKinley for providing me with employment that financially helped carry me through my last two years of study.

TABLE OF CONTENTS

LIST OF TABLES

LIST OF FIGURES

LIST OF PERMITTED COPYRIGHTED MATERIALS

1: INTRODUCTION

The gross morphologies of the skeletal elements that compose human hands/feet and bear (*Ursus americanus*) front/ hind paws look remarkably similar, and they are commonly misidentified as one another. As recently as August 7th, 2009, a hind bear paw had been initially mistaken for a human foot in Ontario County, New York; however through DNA testing it was subsequently found to be most likely the paw of a bear (CBC News, 2009). The similarity is due to both species exhibiting almost identical skeletal elements that articulate in the same fashion. As well, the gross morphologies of these elements show remarkable similarities. Stewart (1959: 19) notes the very same bones represented in human hands are also represented in bear paws (see Figure 1) i.e. carpals, metacarpals and phalanges. As with the similarities of human hands and front bear paws, so too are these similarities displayed between human feet and hind bear paws which are both composed of tarsals, metatarsals and phalanges.

Studies addressing whether the skeletal similarities observed among human and black bear elements at the gross morphological level are also present at the microscopic level are lacking within the literature. Specific research providing quantitative data for bear bone is scarce in the current literature, and J. S. Foote (1916) is one of the only researchers who has examined cortical bone in bears (Hillier and Bell, 2007).

The remarkable similarity among the skeletal elements of human hands/feet and bear front/hind paws is interesting, and perhaps even puzzling from a biomechanical point of view because each species displays completely different modes of locomotion; humans are bipeds whereas bears are quadrupeds. The structure and shape of bone is a reflection of its function within the skeletal system of an organism which includes

structural, protective, support and locomotor components. In skeletal structures, architectural differences exist between the morphological features of human and

Figure 1.1 Photograph depicting the skeletal similarity between a human hand (left) and black bear paw (right) (Source: Sims, 2007: 3) Permission to reprint granted by author and publisher.

nonhuman bone. Byers (2008: 62) explains that "quadruped mammals share similar bone architecture due to their four-footed stance, as opposed to humans who display a bipedal stance and have their own unique architecture." Komar and Buikstra (2008: 76-77) also note that "the differences in mode of locomotion present among human and nonhuman species is reflected in bone morphology; human bipedalism is reflected in virtually every element of the human body, whereas quadruped mammals exhibit such features as the posterior placement of the foramen magnum and the elongation of the pelvis."

Due to the fact that a species' skeletal morphology is a reflection of a species' mode of locomotion, it is relevant to ask why the skeletal elements from human hands/feet look so similar to those of bear front/hind paws when humans are bipeds and bears are quadrupeds? If morphological features differ between human and nonhuman

bone due to architectural differences resulting from different modes of locomotion, one would expect human hands/feet and bear front/hind paws to look different from one another, not alike. Why, then, are they so alike?

This peculiar case of similar skeletal morphology between two species that exhibit different modes of locomotion, serves as the basis to investigate: 1) whether biomechanical loading due to a species' mode of locomotion affects microscopic bone structure and form, 2) whether microscopic bone morphology (as opposed to gross skeletal morphology) in fact provides a more accurate and representative method to infer a species' mode of locomotion, and finally 3) to assess whether these microscopic morphologies can be accurately observed and analyzed non-destructively, through the use of microcomputed tomography imaging (Micro-CT).

Specifically, this thesis will analyze biomechanically regulated microscopic cortical bone structures (i. e. cortical porosity, canal number, canal diameter and polar moments of inertia) of the third metacarpals (MCs) and metatarsals (MTs) for both human hands/feet and black bear front/hind paws to assess the hypothesis that differences in the microscopic bone structures between human hands and bear front paws will be present due to the fact that bears use their forelimbs for locomotion, whereas humans do not. Similarities are expected in the microscopic bone structures between human feet and bear hind paws because both species use these particular elements in a similar fashion, specifically for locomotion. Results from this analysis, along with the striking gross skeletal morphologies observed among bear and human third digits, are expected to provide support for the argument that comparative bone morphology, which is commonly

used to define an individual's mode of locomotion, needs to be analyzed at the microscopic level.

The analysis and comparison of the microscopic bone morphologies between human elements versus bear elements to infer the relationship between mode of locomotion and microscopic skeletal morphology could have profound implications for evolutionary researchers who infer ancient hominin locomotion patterns based on the gross skeletal analysis of fossil morphology. The emergence and development of obligate bipedal locomotion is one of the most significant structural adaptations to have occurred among ancient hominin species, and it has subsequently become one of the most intensively investigated evolutionary trends. As discussed below, evolutionary theories addressing various aspects of the emergence of bipedalism have concentrated on the gross skeletal morphologic analysis of postcranial elements of humans and closely related species, both for extinct and extant taxa. For example, Harcourt-Smith and Aiello's (2004) review of human evolutionary bipedalism via the skeletal anatomy of the foot of numerous hominin species proposed that different foot morphologies, and thus different adaptations to bipedalism, equate to different species inhabiting different areas, even at a similar point in time. This assumption that a species' mode of locomotion may be characterized strictly through their gross skeletal morphology may in fact be misleading because quadrupedal black bears and bipedal humans show remarkable gross skeletal similarities.

Through the advent of advanced imaging technologies such as three-dimensional Micro-CT, accurate 3D representations of the natural 3D properties of bone are now achievable. One of the most significant features of Micro-CT is that it is a completely

non-invasive tool that can be used for analyzing the microscopic characteristics of sensitive materials such as human and ancient fossil remains which could prove to be invaluable for evolutionary researchers who attempt to define the locomotor repertoires of ancient hominins. Answers to understanding bipedalism and how we as humans came to be the only fully obligate species at present lies at the heart of hominin evolution.

1.1 Thesis organization

This thesis will be organized into five chapters. Chapter two will provide a brief review on bipedalism research through the comparative anatomy of skeletal structures involved in bipedalism, specifically the foot, including both extinct and extant taxa. Technological approaches used to describe the morphological characteristics of a species' mode of locomotion will be explained through the concepts of biomechanics and the mechanical properties of bone. Finally, specific cortical bone structures proposed as indicators of biomechanical stressors will be presented.

Chapter three will present the specimens utilized for this research along with an introduction to both 2D and 3D techniques implemented for the assessment of bone mechanical properties. Specifically, the application of 3D Micro-CT and 2D histology used to describe cortical bone structures such as cortical porosity, canal number populations, canal diameter and finally the geometric parameter polar moments of inertia will be presented. Lastly, the protocols used for Micro-CT and histology analysis will be described.

Chapter four will present the quantitative data obtained from both 3D and 2D analysis and the statistical testing used to compare and contrast the microscopic cortical structures of human elements versus bear elements in relation to biomechanical loading

due to each species mode of locomotion. Statistical testing will also be used to compare methodology, specially the quantitative data obtained for like structural characteristics from 3D Micro-CT and 2D ground histology. Qualitative analysis of histology sections will also be presented. Chapter five will present conclusions, study limitations and future directions for analysis.

2: RESEARCH CONTEXT

2.1 Overview of research on bipedalism

The emergence and development of obligate bipedal locomotion is one of the most significant structural adaptations to have occurred among ancient hominin species, and it has subsequently become one of the most intensively investigated evolutionary trends. Significant hominin fossil discoveries such as *Australopithecus afarensis* AL 288-1 (a.k.a. "Lucy") and *Ardipithecus ramidus* (ARA-VP-6/505) revolutionized how archaeologists and anthropologists interpret and identify ancient hominin lineages within evolutionary history. Because the anatomy of bone, specifically its skeletal structure and shape, is a reflection of its function within the skeletal system, hominin fossil remains provide researchers with the ability to directly observe and compare hominin gross skeletal morphologies as a means to infer a species' mode of locomotion. The ability to investigate fossil materials not only provides a means to interpret ancient hominin locomotion, but also furthers our own understanding of how we, *Homo sapiens*, evolved to become the only fully obligate bipedal species of present. The following sections attest to the importance of hominin fossil remains for furthering our understanding of bipedalism and, thus, mode of locomotion.

Comparative osteology of both extant and extinct taxa has proven to be an invaluable analytic tool for the investigation of theories that attempt to answer the "big picture" evolutionary questions in terms of how, when and why a bipedal mode of locomotion came into existence (Harcourt-Smith and Aiello, 2004). For example, the discovery of fossil remains of *A. afarensis* (AL 288-1) included complete elements from the forelimb and hindlimb; specifically the humerus and femur; respectively (Jungers,

1982). These skeletal elements were significant because they provided researchers with more comparative and comprehensive information with which to test the biomechanical properties of the postcranial elements of hominin species and thus to infer mode of locomotion. Jungers (1982) stated these remains provided researchers with "the first opportunity to test previous inferences about limb proportions and skeletal allometry in ancient hominids" (Jungers 1982: 676), which up to that point in time had not been substantially understood from a biomechanical analytical viewpoint (Walker 1973: 554).

Subsequent hominin fossil discoveries such as *A. ramidus* (ARA-VP-6/505) further attest to the significance of comparative osteology to infer mode of locomotion. Prior to *A. ramidus*, it was a common assumption that "our foot evolved from one similar to that of modern African apes" (Lovejoy et al., 2009: 72). Unlike *A. afarensis* (AL 288-1), *A. ramidus* (ARA-VP-6/505) provided elements of well preserved foot bones which included: "a talus, medial and intermediate cuneiforms, cuboid, first, second, third and fifth metatarsals and several phalanges" (Lovejoy et al., 2009: 71). The gross morphological analysis of *A. ramidus*' (ARA-VP-6/505) foot elements against those of modern apes led Lovejoy et al. (2009) to conclude that the bipedal adaptation of *A. ramidus* (ARA-VP-6/505) did not follow a linear and immediate successive pattern from a previous bipedal hominin species; instead, it exhibited elements of both arboreal and terrestrial locomotion patterns from species with less extensive locomotor repertoires.

Without the fossil remains of ancient hominins such as the two aforementioned species, detailed comparative investigations of the various attributes of bipedalism is not possible, and it will be argued below that skeletal anatomy is a crucial parameter in the determination of mode of locomotion.

2.2 Review of modern comparative gross anatomy of hominin locomotion

Research on hominin postcranial elements (Lovejoy et al. 2009; Harcourt-Smith and Aiello, 2004) has provided a wealth of insight into the factors surrounding the emergence and evolution of a bipedal mode of locomotion through the analysis of the gross skeletal morphologies of both extinct and extant taxa. Although specific skeletal features such as the placement of the foramen magnum on the basicranium region of the skull and the shape and placement of the pelvis are commonly known as indicators of a species' mode of locomotion, more recently another feature of the skeleton has been included within this group of skeletal indicators – the foot.

2.2.1 Inference of locomotion through skeletal analysis - anatomy of the foot

The argument that the anatomy of the foot is paramount to infer a species' mode of locomotion (Pontzer et al. 2010; Lovejoy et al. 2009; Marchi, 2005; Harcourt-Smith and Aiello, 2004; Berillon, 2003) is based upon the fact that it is the "only structure that directly interfaces with the ground, and subsequently is under strong selective pressure to deal with both balance and propulsion in a highly efficient way." (Harcourt-Smith and Aiello, 2004: 404). In other words, during locomotion, the foot becomes a multi-functional system in which the bones articulate with one another in a particular fashion that facilitates both the locomotor repertoire of an organism while simultaneously supporting their skeleton. Harcourt-Smith and Aiello (2004: 404) state, "Increased knowledge therefore about the relationship between the structure and function in the foot bones of our hominin ancestors, as well as extant primates, is central to our understanding of the origins and evolution of bipedalism."

2.2.1.1. Skeletal comparison of extinct taxa. Foot morphology has become increasingly prominent in the investigation of bipedal evolution. While the ability to infer ancient hominin species' modes of locomotion directly from their gross skeletal anatomy is clearly advantageous, it is not necessarily clear cut and straight forward.

Harcourt-Smith and Aiello's (2004) review of the evolution of bipedalism attests to the discrepancies among researchers in regards to determining species' modes of locomotion identified through comparative gross skeletal morphology. For example, comparison of the foot bones of *A. africanus,* Stw 573 (a.k.a. Little Foot) and *H. habilis,* (OH8) showed their skeletal anatomies to be different from one another; however, the opposite was observed in that their body proportions were similar, resulting in a conclusion that different forms of bipedalism were likely emerging from different hominin lineages. (Harcourt-Smith and Aiello, 2004)

Harcourt-Smith and Aiello's (2004) review further showed that analyzing the gross morphologies of ancient hominin species can be even more problematic when hominin bipedal traits are based on analyzing several individual elements of the foot that result in conflicting estimations of locomotor modes between seemingly similar species. Clark and Tobias (1995) argued that the gross anatomy of the talus for both *A. africanus* and *A. afarensis* were similar in morphology, thus indicating a common mode of locomotion for these two particular hominins; however, in a study by Latimer and Lovejoy (1990) evident differences in the opposability of the halux for *A. africanus* and *A. afarensis* actually led to the conclusion that each species displayed a different locomotor mode. Based on the substantial comparative analysis of ancient hominin fossil

remains, in particular the comparative anatomy of the foot, Harcourt-Smith and Aiello (2004: 412) concluded:

> What emerges is that the overall picture is highly complex, and implies that different taxa living in different parts of Africa, but at a similar point in time, were most likely to have had feet that represent a mosaic of human-like and ape-like morphologies, but that these mosaics were different to each other, implying qualitatively different modes of bipedalism.

2.2.1.2 Skeletal comparison of extant taxa. The previously discussed studies addressed bipedalism of extinct hominins, but foot morphology has also been compared in modern extant species as a means to infer the locomotor patterns of extinct taxa. In a study by Marchi (2005) the skeletal morphology of the foot for both extant great apes and modern humans was utilized as an indicator for a bipedal mode of locomotion. Specifically, Marchi (2005) assessed the plausibility of a relationship between locomotor mode and the cross-sectional diaphysis dimensions of the MCs and MTs of extant great apes and modern humans.

Marchi (2005) proposed that the way in which loads are accommodated by extant species during locomotion could be inferred and could therefore provide researchers with a means to infer the locomotor modes of ancient hominin species. Interestingly, Marchi (2005) did find that the cross-sectional parameters of the MCs and MTs of like digits in human and great ape serve as good indicators of general locomotor patterns, so implementing this form of skeletal analysis could actually contribute to a better characterization of the locomotor patterns of extinct primates.

2.3 Technological approaches to skeletal morphology analysis of bipedalism

Utilizing gross morphology characteristics of bone such as cross-sectional parameters has been shown to serve as useful indicators for inferring a species mode of

locomotion (Marchi, 2005). However, through the comparison of skeletally similar elements of black bears and humans, it is argued that a strictly gross morphological analysis may not necessarily provide a comprehensive and accurate assessment of species' modes of locomotion. Undeniably, bears and humans display different modes of locomotion; bears are quadrupeds whereas humans are bipeds. As well, each species has markedly different weight ranges. It could be assumed these factors would affect the biomechanical forces exerted on these species' skeletal elements and thus affecting their skeletal structures as showing differently from one another, however interestingly this is not observed at the gross morphological level.

The previously discussed bipedalism studies emphasized the significance of assessing species' gross skeletal morphologies to infer modes of locomotion. However, from the example of remarkable gross skeletal similarity among two species that exhibit different modes of locomotion (i. e. quadrupedal black bears and bipedal humans), a microscopic analysis of cortical bone structure is proposed as a more accurate means to determine a species mode of locomotion via the affects that biomechanical loading due to locomotor mode imposes on bone structure and shape.

Through the microscopic analysis of the third MCs and MTs of bear elements versus human elements' microstructures, typically described as affected by the biomechanical forces exerted upon them, it is then possible to investigate the extent that biomechanical loading dictates bone structure and shape as a result of mode of locomotion and whether microscopic bone analysis is a more efficient method of inferring one's mode of locomotion.

2.3.1 Concepts of biomechanics

To fully appreciate how biomechanical forces alter and affect the structure and shape of bone, a brief review of the mechanics behind these forces is presented. Nordin and Frankel (2001: 3) describe the discipline of biomechanics as one that utilizes the basic properties of classical mechanics to analyze biological and physiological systems. At a very basic level, biomechanics strives to answer how objects work; both from the perspective of an object's own physical properties and the physical properties of the forces acting upon it. Specifically for this study, the mechanics of solids within biological systems will be used as a reference point to investigate and compare the microscopic skeletal morphologies of the third MCs and MTs for both humans and bears to identify the biomechanical forces exerted as a result of each species' mode of locomotion.

Some basic biomechanical concepts are particularly useful in explaining skeletal morphology with the understanding that various loading modes can and do alter and change the shape of bone. The alteration of the local shape of an object or its "deformation" occurs when externally applied forces cause an object in a state of "static equilibrium" to conform in the direction of the net force acting upon it (Nordin and Frankel, 2001: 7). How an object reacts or deforms to an externally applied force can be used as an indicator to identify the type of force, or loading mode, acting upon it (Nordin and Frankel, 2001: 7).

Nordin and Frankel (2001) provide an excellent explanation of the basic forces observed within the discipline of biomechanics and how each of these affects an object's local shape, which I will summarize in the following. Tension can be described as a force that results in the "pulling" or lengthening of an object's body upon application of a

force. Compression is the opposite of tension, where the application of a force causes an object to collapse or shorten towards the force acting upon it. In shear loading, forces are acting against one another located at an area of a structure that is resisting the force being applied. Bending and torsion cause objects to deform based upon the moment and torque actions of the forces being applied. Bending and torsion are especially informative in regards to skeletal loading, which will be discussed in further detail in Chapter three. It is also important to note that these aforementioned forces do not necessarily act individually from one another but can act upon an object simultaneously, resulting in a combination of loading affects (Nordin and Frankel, 2001: 7).

2.3.2 Structural anatomy of bone

To investigate how biomechanical forces affect microscopic bone structure and shape, and how bone tissues react and respond to such forces, it is important to understand not only the nature of the forces exerted upon bone resulting from one's mode of locomotion but also to understand how the structural properties of bone itself, particularly bear and human bone in this case, respond to such forces structurally. The structural properties of bone can be examined and assessed through histological analysis. Histological analysis involves the examination of the appearance of thin and block sections of bone tissue to provide a way to quantify (known as "histomorphometrics") the histological structures within tissue (Hillier and Bell, 2002: 249).

2.3.2.1 Bear bone anatomy. Specific research on the histology of bear bone is scarce in the current literature, and J.S. Foote (1916) is one of the only researchers that have examined the cortical bone in bears. Foote (1916: 107-108) studied the femoral section of a black bear (*Ursus americanus*, see Figure 2.1) and identified the following features:

1) short and long laminae having a general concentric arrangement but presenting a variety of positions in the different portions of the wall, 2) the anterior and outer wall laminae are either short and long, showing curvature of the bone, or present and short angular curves that run transversely. Foote (1916) also notes that the laminae are quite uniform in width and are separated by distinctly wide canals. In the posterior wall the laminae are interrupted by a few Haversian systems that are well developed. Also, in the inner wall the laminae are more uniformly concentric (Foote 1916).

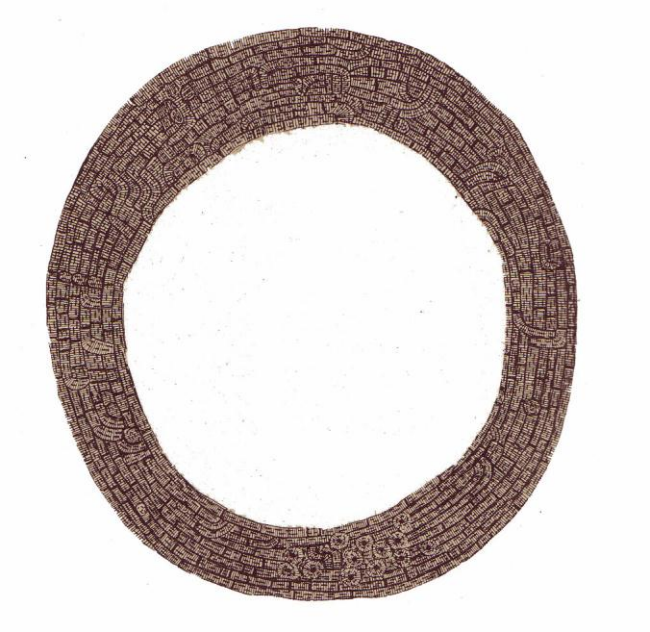

Figure 2.1 Foote's (1916) Illustration of a Bear Femur Section (Source: Foote 1916: Figure 209, Plate 12)

The morphologies of the skeletal elements of bear and human paws/hands/feet are very similar at the gross level however, differences are discernable at the microscopic level; specifically, nonhuman bone contains a type of bone called plexiform bone. Plexiform bone is defined by its "horizontal, regular, and rectangular organizations and is typically found in nonhuman mammalian bone" (Mulhern and Ubelaker 2001: 220).

Although this type of bone can be found in human bone, specifically in young human bone, it is very rare (Mulhern and Ubelaker 2001: 220).

2.3.2.2 Human bone anatomy. Human bone is composed of a vast and intricate array of co-mingling chemical, microscopic, and morphological systems. These systems coincide with one another to form the final product: bone. For the purposes of this research one of these systems, Haversian systems, which are also referred to as secondary osteons, will be concentrated on due to their important roles in assessing biomechanical loading as a result of mode of locomotion.

Haversian bone morphology is an important characteristic in regards to interpreting the biomechanical behaviour of bone. Steele and Bramblett (1998) provide a comprehensive explanation on Haversian bone anatomy which is summarized as follows. Haversian systems are described as the "unit of bone microstructure consisting of a nutrient (or Haversian) canal and the surrounding concentric lamellae" (Steele and Bramblett, 1998: 267). These concentric lamellae that surround each Haversian canal consist of small structures known as lacunae, which are responsible for housing bone forming cells known as osteocytes. Canaliculi are the structures that serve as bridges for the lacunae, connecting them to one another. Steele and Bramblett (1998:10) note, "this complete system consisting of the Haversian canal and its related lamellae is known as the Haversian system or secondary osteon." Mulhern and Ubelaker (2001: 220) also state that "secondary osteons, or Haversian systems, are discrete bundles of lamellar bone surrounding a Haversian canal and are defined by a cement line."

2.3.3 Adaptive mechanical properties of bone

It has been widely noted within the literature that biomechanical forces greatly influence and/or govern the shape and arrangement of bone (Seeman, 2008; Basillais et al. 2007; Seeman and Delmas, 2006; Chen et al. 2004; Skedros et al. 2004; Skedros et al. 2003; Burr et al. 2002; Turner, 1998; Currey, 1984; Laynon, 1984; Laynon and Baggott, 1976) and in turn, the mode of locomotion an organism exhibits also greatly affects the appearance and structure of bone. Bone is unique in that it is a complex and dynamic tissue that continually renews itself throughout life, and has the ability to respond and adapt to the mechanical demands and stressors placed upon it. Nordin and Frankel (2001: 27) describe bone as follows: "A highly vascular tissue, it has an excellent capacity for self-repair and can alter its properties and configuration in response to changes in mechanical demand."

How bone reacts under the influence of forces, also known as its "mechanical behaviour", is determined by a number of properties, including "its geometric characteristics, the loading mode applied, direction of loading, rate of loading, and frequency of loading" (Nordin and Frankel 2001: 36). These basic structural properties of bone result in a complex and dynamic skeletal system that carries out many tasks, some of which include: "protection of internal organs, providing rigid kinematic links and muscle attachment sites, and facilitating muscle action and body movement" and it is these unique characteristics of bone that allow it to carry out these specific tasks (Nordin and Frankel 2001: 27).

In particular, the stiffness and strength of bone to withstand but also react to biomechanical forces while maintaining its various functions within an organism is a significant mechanical property of bone (Seeman, 2008; Seeman and Delmas, 2006;

Currey, 1984; Jungers and Minns, 1979). For optimal function within an anticipated environment, the gross shape of a bone is contained within its genetic makeup; however, the reverse of this, loading determines a bone's structure and the capacity to react to these loads, is also a requirement for optimal functionality (Seeman, 2008). The natural strength of a bone, which is its ability to bear a load before it breaks, is its most important mechanical attribute. It depends on, "the stiffness and strength of the bone material itself and also the build of the whole bone", which is the amount of bone material present and how it is spatially distributed (Curry, 1984: 4).

The stiffness of a bone can be viewed of in terms of how "elastic" it is. In biomechanical terms, the elasticity of an object is defined as the capacity to resume its overall shape and size after an applied load has been removed (Nordin and Frankel 2001: 10). Elastic materials have a maximum amount of stress-strain that can be tolerated before they completely fail. This elastic behaviour of materials, including bone, can be understood through stress-strain diagrams. Nordin and Frankel (2001: 11) note, that if a material's stress-strain diagram displays as a straight line, then that material is said to be linearly elastic in that the stress and strain endured are proportional to one another and that the slope of the diagram represents the elastic region of the material. This elastic region is known as the Young's modulus (E) of the material in question.

The other factor that affects bone stiffness is its "plasticity" which is the result of a material being loaded past its elastic limit (yield strength), resulting in permanent deformation, and if the load is continually increased beyond this yield strength limit, the end result will be complete fracture (Nordin and Frankel 2001: 11). A very simple example that encompasses elasticity and plasticity is a rubber band, it can only be

stretched so far until it is beyond its capacity to return to its original form and therefore breaks.

The fact that bone maintains stiffness and strength simultaneously is quite remarkable since these two structural features are in a sense contradictory to one another. Seeman and Delmas (2006: 2250) explain bone must be multi-functional; stiff enough to facilitating loading but still resistant to deformation by narrowing and lengthening its shape, while at the same time, flexible enough to facilitate energy absorption by actually deforming to compression and tension forces by shortening and widening its shape. Therefore, if bone is structurally too stiff and lacks the ability to give, the end result is structural failure – initially observed through the development of microcracks to complete failure or fracture (Seeman and Delmas, 2006). Nordin and Frankel (2001) assert that administering an externally applied force or load that is known to deform the overall structure and shape of a bone provides an efficient means to infer a bone's mechanical behaviour, and thus its mechanical stiffness and strength.

2.3.3.1 Bone design – gross morphology. The overall design of the types of bones found within the skeletal system (i.e. short, long, flat, and irregular) is a reflection of their specific functions within this system and of their anticipated mechanical behaviour. Stout (2003), Jaworski (1976) and Enlow (1975) and Hillier and Bell (2007: 252) explain that while different types of bone, such as flat (cranial) and short (vertebra), contain the same histological structures as long bones, their histological appearance may differ which is proposed as being a result of the biomechanical forces acting upon them. For example, the "hollow tube" shape of long bones facilitates superior strength and durability against compressive forces while simultaneously minimizing the over-all weight of the bone

required to achieve this task (Sommerfeldt and Rubin 2001: 90). Lanyon (1984: 56) also states, "In bones whose predominant function is load-bearing, rather than protection or display, the particular features on which structural competence depends all require functional activity for their development."

2.3.3.2 Bone design – cortical and trabecular tissue. Tubular long bones are comprised of two major bone tissues; cortical and trabecular bone. Macroscopically, cortical bone is the dense compact bone comprising the walls of the shaft, also known as the diaphysis, in the long bones as well as the exterior surface of other bones. Trabecular bone differs from cortical bone in that it is highly porous and arranged in a lattice or honeycomb-like pattern, and due to its appearance, it is sometimes referred to as "spongy" bone. Trabecular bone is found in the ends of long bones, the vertebral bodies and the interior of cranial bones and other flat bones.

Both cortical and trabecular bone play an important role in the overall mechanical behaviour of bone. The architectural structure and arrangement of trabecular bone in relation to bone strength has become a common and well documented relationship (Hanson and Bagi, 2004; Carter et al. 1996; Bartlet et al. 1966). This relationship between the architectural parameters of trabecular bone in relation to bone strength has further been used to suggest that the structural characteristics of cancellous bone reflect the loading history of bone (Fajardo et al. 2002: 2). Borah et al. (2001) also state that trabecular bone can be used as an indicator of the load bearing capacity of bone

Studies on trabecular bone architecture in relation to biomechanical loading are extensive, having been investigated "since the mid- to late-1800's" (Fajardo et al. 2002: 1) yet, far fewer investigations have been carried out on the microscopic structures of

cortical bone in relation to mechanical behaviour. As stated by Basillais et al. (2007: 141), the incorporation of cortical bone studies in relation to bone strength is necessary because it "represents 80% of the skeleton bone mass and therefore contributes to mechanical bone strength." The long bones then become of particular interest in terms of inferring the structural and geometric properties of bone associated with its mechanical behaviour as the majority of cortical bone is located within them (Augat et al.1996). The significance of investigating cortical bone within long bones is also noted by Cole and van der Muelen (2011: 2141), Gross et al. (1992), Biewener (1991) and Laynon et al. (1975) due to high levels of "stress and strain" endured primarily as a result of forces that "induce bending and torsion."

Cortical and trabecular bone respond differently to loading. Cancellous bone acts as a distributor of loading, transmitting forces from joint surfaces to the cortex, whereas the cortical bone located in the diaphysis of long bones absorbs loading because it actually experiences the greatest loads and thus deformations (Cole and van der Muelen, 2011). Therefore, cortical bone is an important factor in providing strength and rigidity to enhance a bone's overall biomechanical loading capacity and the ability to resist structural failure.

2.3.3.3 Bone adaptation characteristics – cortical modeling and remodeling. Bone is a complex and dynamic three-dimensional material that continually renews itself throughout its lifespan. The characteristics of bone architecture and structure can be viewed at both the macroscopic and microscopic level, and so too can the adaptive processes that result in these characteristics. Frost (1969) was one of the first individuals

to define and measure bone formation processes which can be divided into two main processes; bone modeling and bone remodeling.

Bone modeling is defined as the process responsible for initiating bone resorption and formation in relation to skeletal growth, thus bone modeling defines a bone's overall geometry and size (Frost 1969: 212) and subsequently then, it the process that alters a bone's gross morphology. The means by which bone actively reacts and responds to biomechanical loading endured throughout life is through the adaptive process of bone remodeling. Bone remodeling, as described by Frost (1969: 212), results in the continuous turnover of microscopic lamellar bone for the purpose of altering small changes in size, shape and quantity. This unique characteristic provides bone the ability to continually renew itself by structurally adapting in response to mechanical stimuli and microdamage due to biomechanical loading. Diaphyseal morphology in long bones is the product of a complex remodeling process of tissue deposition and resorption which is believed to be an adaptive response of bone to mechanical stresses and strain (Jungers and Minns, 1979: 285; Hoyte and Enlow, 1966; Enlow, 1963). This notion that argues bone tissue is deposited in relation to mechanical loading and is resorbed in the absence of mechanically induced stressors was first proposed by Wolff (1892) and became known as Wolff's Law.

Both trabecular and cortical bone of the adult skeleton are composed of mature, organized lamellar bone tissue that is a result of the uniform addition of lamellae to bone surfaces during appositional growth, but the specific adaptive process of bone remodeling only occurs within cortical bone (White and Folkens, 2005). In cortical bone, specific structures known as Haversian systems or secondary osteons are present within new,

remodeled secondary bone. The new, secondary bone is formed by bone resorbing cells (osteoclasts) that remove damaged microscopic packets of bone for bone forming cells (osteoblasts) to replace with new bone (White and Folkens, 2005). It is this characteristic of cortical bone first described by Frost (1969) that makes it suitable for investigating the relation between bone tissue structural organization and biomechanical loading. Hillier and Bell (2007: 251) for example, argue that "this remodelling process is typically the result of some factor affecting bone, which can include growth and/or development, injury, strain or something of a pathological nature." Therefore, if a bone in question is not foetal or young in age, and is not afflicted with disease, the presence of Haversian systems indicates that remodeling has taken place in reaction to some form of a biomechanical force such as a load or strain. It is important however, to acknowledge that all bone remodeling is not necessarily mechanically driven or "targeted" and can be excessive beyond what is required to maintain a bone's mechanical capacity (Parfitt, 2002: 7). For example, "nontargeted" remodeling may be a product of characteristics such as hormone levels that result in bone building cells extending beyond their targeted areas (Parfitt, 2002: 7).

2.4 Microscopic cortical structure – biomechanical indicators

Cortical bone remodeling results in the production of Haversian systems and is a bone's mechanism to structurally respond and adapt to biomechanical loads and strains endured throughout life. It can then be proposed that Haversian systems are viable structures to identify the biomechanical forces affecting a particular bone in relation to a particular species' mode of locomotion. For example, Stout (2003) notes that the longitudinal forces that act upon long bones result in longitudinally oriented Haversian

systems, which provide a way to observe the biomechanical forces acting on long bones. Other characteristics of Haversian systems such as their overall shape and populations within defined areas can also be utilized as indicators of biomechanical loading. As bone modeling affects the overall size and shape of a bone during growth to produce skeletal elements that are optimal for meeting the demands of an organism, both from a weight distribution and locomotion aspect, cross-geometric parameters such as moments of inertia that attest to the general mechanical strength of bone, can also be used to infer biomechanical strain.

2.5 Summary

Comparative gross skeletal anatomy is a prominent analytic tool used for inferring species' modes of locomotion because bone structure and shape is a reflection of its function within the skeletal system. Specifically, the relationship between a species' foot morphology and their mode of locomotion is considered crucial as the elements of the foot directly interact with the ground during locomotion. Gross skeletal analyses can and do provide insight into the mechanical characteristics of bone, however they cannot identify correlations between microscopic bone structural responses to locomotion induced biomechanical stress and strain. From the observation of the remarkably similar gross morphologies of the third MCs and MTs of bears versus humans, it is argued that inferring a species' mode of locomotion through the analysis of their skeletal morphology needs to be carried out at the microscopic level in order to obtain a representative identification of a species' mode of locomotion. The methods by which these microscopic bone structures can be used for assessing biomechanical effects will be discussed in further detail in chapter three.

3: MATERIALS & METHODS

3.1 Specimens

The third MCs and MTs from five mature black bears (*Ursus americanus*) and five mature humans were used for both 2D and 3D analysis. Adult human and bear bone was chosen for analysis based upon the presumption that the cortical microstructure would be a reflection of the effects of biomechanical loading, not growth and development. Human bone maturity was based on completely fused epiphyses with no visible fusion lines. Bear bone maturity was based on epiphyseal fusion, as well as age classes that define a sub-adult as 2-3 years in age and an adult as 4+ years in age (Hebblewhite et al., 2003). The third MCs and MTs were selected for analysis under the assumption that, due to their articulation, they would be the digit most likely to evenly carry weight distributions and biomechanical loads, thus providing a more detailed and accurate analysis of bone biomechanical loading factors. It should be noted that sample selection for both human and bear was also based on a lack of visible signs of disease or pathology.

All black bear paws utilized for this research were obtained from Brandon University's Department of Anthropology's Suyoko A. Tsukamoto, who initially obtained the paws from Manitoba Conservation (Permit # WBO8992). Identification information from Manitoba Conservation for each bear includes the age, sex, and tag number (see Table 1). All proper documentation and permits for the possession of black bear remains are found in the appendices (see Appendix A).

TABLE 3.1 Bear paw sample inventory

Tag #	Sex	Approx. Age (years)	Side
SUO901399 GHA 22	Male	3	Right
SUO900436 GHA 24, 19B	Male	4	Right
SUO900441 GHA 24, 19B	Male	4	Right
SUO900802 GHA 23	Female	6	Right
RUO902375 GHA 23	Male	8	Right

The third MCs and MTs from the human sample set were obtained from the University of Manitoba's and the University of Winnipeg's Departments of Anthropology skeletal teaching collections. All human MCs and MTs were from the left side of the body. No specific information on age or sex was available.

3.2 Overview of 2D bone techniques

Traditional testing of a bone's biomechanical characteristics usually involves some form of a mechanical apparatus, and as noted by Mueller (2009: 373), mechanical testing is considered to be the "gold standard method for determining bone competence". For example, loading a bone until it reaches its mechanical limit in an apparatus such as a "testing jig" can be utilized to analyze stress and strain characteristics of a particular bone in question (Nordin and Frankel 2001: 32). While this methodology provides precise data on the mechanical capacities of bone, it is invasive and destructive, destroying the bone specimen for any further testing of a similar nature. Classic mechanical testing does provide quantitative data on how a bone reacts to a biomechanical force as a complete, whole element observed at the gross morphologic level (Mueller: 2009), but it does not reveal how the microscopic structures of bone, such as the Haversian systems, react to biomechanical forces to maintain a bone's optimal functionality, thereby ultimately reducing the probability of failure.

Visualizing and analyzing the architecture and structure of bone morphology at the microscopic level has traditionally been carried out using 2D techniques. Until the advent of sophisticated 3D imaging technology, Fajardo et al. (2002: 1) noted that 2D visualization of trabecular bone morphology was mainly carried out through: "histological thin sections, planar radiography, and conventional computed tomography (CT)", and of these methodologies, only histology enabled the precise characterization of trabecular bone morphology (Merz and Schenk: 1970; Simon and Radin: 1972; Radin et al., 1973; Parfitt et al., 1983, see also Fajardo et al., 2002). While it is common knowledge that histological methodologies do provide a means to quantitatively describe the dynamic structure of bone tissue (Cooper et al., 2003; Parfitt, 1983; Frost, 1969), it also does come with some inherent deficiencies. Ruegsegger et al. (1996: 24) explains:

> Standard histomorphometric procedures have some drawbacks: the invasive nature of bone biopsy technique does not allow longitudinal studies on individuals, the biopsies are destroyed during sample preparation, and the procedure is two-dimensional.

The inherent issues associated with histology become even more evident when analysis involves specimens of a sensitive nature, such as human and nonhuman primate remains (both extant and extinct), potentially making the utilization of histology altogether unrealistic (Fajardo et al., 2002).

3.3 Overview of 3D bone techniques

A particular disadvantage of histomorphology is its inability to visualize and assess bone in its natural 3D state. Bone is a dynamic three-dimensional tissue that continually renews itself throughout life, thus to fully appreciate its microscopic structure and mechanisms, it is crucial to carry out analyses in 3D (Bouxsein et al., 2010; Jones et al., 2004; Cooper et al., 2003; Parfitt et al., 1987). With specific reference to cortical

canals, for example, 2D techniques cannot reveal the 3D nature of these canals as they exist and remodel in 3D, thus requiring a 3D analysis to fully appreciate their structure and characteristics (Basillais et al., 2007; Stout et al., 1999; Cooper et al., 2003). As previously noted, techniques that destructively analyze human and nonhuman primate bones are rarely permissible, therefore the use of non-destructive 3D techniques to assess biomechanical indicators to ultimately explain an individuals' mode of locomotion is invaluable.

The 3D analysis of microscopic bone tissue was formerly limited due to the lack of methodological approaches and technology (Cooper et al., 2003). While stereological techniques can be used to acquire 3D data based on reconstructed 2D serial sections (Parfitt, 1987), it is a very time intensive and cumbersome task (Hanson and Bagi, 2004; Cooper et al., 2003) that destroys the bone for any future analysis. The ability to analyze bone tissue in 3D, however, is now possible through the advent of 3D imaging technology such as micro-computed tomography (Micro-CT). Micro-CT was first introduced as a means to analyze bone microstructure within its natural 3D state by Feldkamp et al. (1989). Bouxsein et al. (2010: 1469) note "micro-CT uses X-ray attenuation data acquired at multiple viewing angles to reconstruct a 3D representation of the specimen that characterizes the spatial distribution of material density."

Compared against traditional 2D histological methods, there are many benefits to using Micro-CT for morphological analysis of both trabecular bone (Muller, 2009; Fajardo et al., 2002; Ruegsegger et al., 1996) and cortical bone (Muller, 2009; Basillais et al., 2006; Chen et al., 2004; Jones et al., 2004; Cooper et al., 2003, 2011; Wachter et al., 2002). A few of the main benefits of utilizing Micro-CT is that bone morphology can be

directly measured as opposed to 2D stereologic techniques that compose 3D data based on reconstructed 2D data, substantially larger volumes of interest (VOI) are obtainable, the acquisition of measures and subsequent results are much faster (Bouxsein et al., 2010). Perhaps the most important feature of Micro-CT analysis is that it a non-destructive, 3D form of analysis which preserves the sample for future analysis.

Micro-CT technology is now considered the "gold standard" for microscopic bone analysis and is continually advancing through higher resolution capacities which in turn allow for the imaging and assessment of smaller and smaller microscopic bone structures. Improvements in resolution have been particularly beneficial for analyzing cortical bone. Cooper et al. (2003: 171) note since its introduction by Feldkamp et al. (1989), Micro-CT has continually advanced through the advent of technology such as synchrotron radiation that can achieve resolutions on the order of 1.4 μm, capable of visualizing minute microscopic structures such as osteocyte lacunae. Commercial systems such as desktop Micro-CT scanners are also continually advancing through increasing resolutions and as cortical canals are naturally much larger structures than osteocyte lacunae; commercial Micro-CT scanners are more than capable of imaging cortical canals in 3D, which previously was unattainable (Cooper et al., 2003: 171). Hanson and Bagi (2004: 326) state that, in general, improvements in the affordability of these systems, advancement in their spatial resolutions, their inherent user friendly operating procedures and the high quality of quantitative data they produce has resulted in their popularity and advancement within the scientific community.

Micro-CT's introduction by Feldkamp et al. (1989) as a means to quantify 3D trabecular bone has significantly paved the road in quantifying 3D bone architecture

(Cooper et al., 2003) including cortical bone architecture. Parfitt et al. (1987) strove to create a universal standardization for practitioners of bone histomorphometry that alleviated inherent semantic barriers as a means to present and interpret data both within and outside the scientific community. In doing so, quantitative characteristics of microscopic trabecular bone tissues were defined from both an identification and analytical standpoint. As noted by Cooper et al. (2003), many of the defined parameters for the quantitative 3D analysis of trabecular bone architecture can be utilized to perform quantitative 3D analysis of cortical bone, given they are measured directly and not based on a structural model. Measurements of these parameters are often achievable using the same analytic software programs that are utilized for trabecular bone architecture analysis. The benefit of this type of analysis is that the microscopic bone structures measured and analyzed are obtained from 3D representations of bone, thus providing an accurate and representative analysis of bone microstructure within its natural 3D environment.

3.4 Application of micro-CT

3.4.1 Cortical porosity (Ca.V/TV, Ca.V/T.Ar)

Defined quantitative 3D trabecular bone architecture parameters can be utilized to quantitatively analyze cortical bone in 3D (Cooper et al., 2003: 171; see Table 3.2). For example, cortical porosity (Ca.V/TV), which is a reflection of the volume of porous canals (Ca.V) within a given tissue volume (TV) (Cooper et al., 2003) is a useful determinant for evaluating the effects of biomechanical loading upon cortical bone because it is noted as a major indicator of bone strength (Basillais et al., 2007; Wachter et al., 2002). Cooper et al. (2004) explain that the mechanical characteristic of cortical bone

TABLE 3.2 Analogous morphological parameters for trabecular and cortical bone*

Trabecular Bone	Cortical Bone
Tissue Volume (TV)	Tissue Volume (TV)
Bone Volume (BV)	Canal Volume (Ca.V)
Bone Surface (BS)	Canal Surface (Ca.S)
Bone Volume Fraction (BV/TV)	Cortical Porosity (Ca.V/TV)
Bone Surface to Tissue Volume (BS/TV)	Canal Surface to Tissue Volume (Ca.S/TV)
Trabecular Thickness (Tb.Th)	Canal Diameter (Ca.Dm)
Trabecular Separation (Tb.Sp)	Canal Separation (Ca.Sp)

*All abbreviations are based upon standard nomenclature (Parfitt et al., 1987) (Cooper et al., 2003). Permission to reprint granted by author and publisher.

is a factor of the area that these pores inhabit within a specific area of cortical bone. The effects of cortical porosity on a bone's mechanical strength can be explained as the more porous the cortical bone is, the weaker the overall mechanical strength of the bone will be. It should be noted as well that Ca.V/TV represents 3D, whereas Ca.V/T.Ar represents 2D measures for cortical porosity.

3.4.2 Canal number (Ca.N)

The number of canals present within a ROI can also be used as an indicator of biomechanical loading. In a study investigating the cortical bone organization of Rocky Mountain mule deer, Skedros et al. (2003) found that populations of Haversian systems and thus canals, increased within the more distally located forelimb long bones suggesting these bones experienced a higher rate of bone remodeling. Skedros et al. (2003) were not able to identify the direct causal mechanisms to explain their findings however, trends such as increased secondary osteon populations in distally located bones have been suggested as a result of the changes in the mechanical stress a bone endures in relation to its function within the skeletal system. This higher remodeling rate Skedros et al. (2003) found was proposed to be a result of an increase in bone loading, creating more microcracking within bone, thus initiating the need for an adaptive or preventative

response to biomechanical forces in the form of bone remodeling (Skedros et al., 2003). Sommerfeldt and Rubin (2001: 91) also support this characteristic of bone remodeling noting its function is to not only to replace dead or damaged tissue, but also to provide bone with the ability to adapt to changes in loading.

3.4.3 Geometric parameters – polar moment of inertia (MMI)

Numerous studies have implemented cross-sectional geometric parameters to define cortical bone strength (Cole and van der Muelen, 2011; Cooper et al., 2007; Kontulainen et al., 2007; Bagi et al., 2006; Marchi, 2005; Cooper et al., 2004; Jungers and Minns, 1979) because a bone's geometry greatly influences its mechanical behaviour (Nordin and Frankel, 2001). Nordin and Frankel (2001) provide a good explanation of these geometric parameters which is summarized as follows: In reference to tension and compression, the cross-sectional area of a bone is directly related to its stiffness characteristic and thus its load to failure property, explainable through the notion that the larger the cross-sectional area, the stronger and stiffer it will be. In bending, a bone's mechanical behaviour will be affected by both the cross-sectional area and the distribution of bone tissue around a neutral axis. These two factors in the bending characteristic of bone can be quantified by the area moment of inertia where the larger the moment of inertia, the stronger and stiffer the bone will be. As in the bending characteristic of bone, bone stiffness and strength in torsional loading are also directly related to cross-sectional area and bone distribution around a neutral axis which are quantified by the polar moment of inertia (MMI), where the larger the polar moment of inertia, the stronger and stiffer the bone will be (Nordin and Frankel 2001: 47-48).

3.5 Application of 2D histology for comparison of 3D micro-CT

While micro-CT is presented as a beneficial analytic tool to non-destructively obtain 3D bone morphometric data, traditional 2D histomorphologic analysis can be used as a tool of comparison to attest to the quality and accuracy of the 3D micro-CT data. For example, Hillier and Bell (2007: 252) explain that "while different types of bone, such as flat (cranial) and short (vertebra), contain the same histological structures as long bones, their histological appearance may differ which is proposed as being a result of the biomechanical forces acting upon them." Longitudinal forces that act upon long bones result in longitudinally oriented Haversian systems which therefore, provide a way to observe the biomechanical forces acting on long bones (Stout, 2003).

Skedros et al. (2003) noted that a higher number of Haversian systems were present in the more distal long bones of Rocky Mountain mule deer, suggesting a higher rate of remodeling potentially due to increased mechanical stress and thus an overall increase in loading. The populations of canals measured in 2D among the site specific ROIs can be therefore be used as an indicator of loading on a bone.

Stout (2003: 240) explains that long bones commonly exhibit relatively round osteons because osteon formation tends to parallel the direction of the major biomechanical force exerted on a skeletal element. Stout (2003: 240) also notes that due to a long bone's weight-bearing role, biomechanical forces are dispersed in a roughly longitudinal orientation which in turn affects the shape of the osteons bearing this force. Therefore qualitative observation of the shape of osteons and canal size can be used to identify whether the shape of bone structures are indeed a result of applied biomechanical forces. Micro-CT has the ability to identify canal diameter (Ca.Dm) which is an analogous parameter to trabecular thickness (Tb.Th), thus the mean of the areas of the

Haversian canals acquired in 2D can be compared against the means of the canal diameters (Ca.Dm) acquired in 3D to validate the equivalency of this measure.

3.6 micro-CT procedure

3.6.1 SkyScan 1172 desktop micro-CT protocol

For consistency, micro-CT slices will be referred to as slices, and ground thin sections will be referred to as sections (Kuhn et al., 1990). All human and bear bone samples were scanned in a SkyScan 1172 (Kontich, Belgium) desktop X-ray microtomograph (<5 µm source spot size; 8.83 camera pixel size) at the University of Saskatchewan's Department of Anatomy & Cell Biology under the supervision of Dr. David M. L. Cooper. The scan protocol utilized a camera offset mode at a rotation step of 0.10 degrees, standardized X-ray settings set at 100kVand 100µ and an exposure time of 0.2 seconds per frame. Prior to scanning, a scalpel blade was used to make a small cut on the superior surface of each bone to maintain its orientation for image analysis and subsequent 2D thin sectioning. This cut on the superior surface was also used to aid in positioning the bone for scanning. The human sample averaged a scan time of 2.19 hours; bear sample averaged 2.49 hours.

Due to the differences in bone density between humans and bears, the cortical canals in the bear sample were more challenging to visualize, so specific filtering protocols were used for each species (SkyScan hardware/software). For the human sample, a 0.5mm thick aluminum filter and a beam-hardening correction of 49% was employed to reduce beam-hardening artefacts. For the bear sample, the maximum level of filtering was implemented by using both an aluminum and copper filter to aid in bone contrast. To account for the filter change in the scan protocol, a flat field optimization

procedure was implemented before the bear sample set was scanned. This essentially corrects the images recorded by the camera by accounting for any deviations in the X-ray source or camera for a particular setting.

3.6.2 micro-CT scan analysis

Each scan for both the human and bear sample set produced 2,159 slices with a resolution of 4µm (2, 159 slices = 8.622 mm). After each scan, a subset of slices was selected for reconstruction. These smaller reconstructed subsets drastically reduce the time required to 3D reconstruct the scan images as well as decrease the file sizes for image analysis. CTAnalyzer (CTAn) version 1.11.1.0 (SkyScan software) enables 3D visualization of micro-CT scans and bone morphometric analysis in both 2D and 3D and was used for all micro-CT image analysis. CT Volume (CTVol) version 1.11.1.0 (SkyScan software) enables 3D surface renderings of the 2D ROIs.

For each human and bear MC and MT, a medial, lateral, superior and inferior circular region of interest (ROI) was extracted from the reconstructed scan set, creating a 3D volume of interest (VOI) that produced 3D quantitative data for the comparison of cortical bone biomechanical indicators; specifically cortical porosity, canal number, canal diameter and area and polar moments of inertia. To produce comparable ROIs, a quadrant mask macro (ImageJ; http://rsbweb.nih.gov/ij/) divided each scan set into four regions related to the anatomical orientation of the bone on which the circular ROI was extended from the periosteal to the endosteal surface of the cortical bone (see Figure 3.1).

Visualization of the cortical canals was achieved by implementing a standardized global threshold for both the human and bear sample set (CTAn software). Measurements of 3D and 2D cortical porosity and canal diameter and 2D polar moments

of inertia were directly acquired from the CTAn results. Ca.N was calculated based on the CTAn data. A 2D Ca.N count consisted of counting the number of pores in each micro-CT slice relative to the cross-sectional area of the VOI, whereas a 3D Ca.N count involved taking the inverse of the sum of the canal diameter (Ca.Dm) and the canal spacing (Ca.Sp) (Cooper et al., 2007).

3.7 Histology procedure

Two individual bear specimens and two individual human specimens were used to produce ground sections of the same areas micro-CT scanned. Due to the small sample size, the 2D thin-sections served as a visually qualitative component to the quantitative micro-CT scans. The 2D sections were visually matched to the corresponding area that was micro-CT scanned, thus, qualitative comparison between the slices and sections facilitated insight into the accuracy and consistency of utilizing micro-CT for microscopic bone analysis. The sections also allowed for the qualitative observation of osteonal shape, which, as previously noted by Stout (2003), is proposed as an indicator of the biomechanical forces exerted upon a bone. Canal populations, canal diameters and the presence and subsequent amount of primary and secondary bone among the ROIs was also qualitatively compared both between and within species and element As well, the general orientation of the Haversian systems, noted by Skedros et al. (2003), is a reflection of biomechanical loading and was visually investigated.

3.7.1 Thin section procedure

Bone sections were cut on a low speed diamond wafering saw (Buehler, Lake Bluff, USA) and cleaned in a distilled water/detergent solution and left to air dry for 24 hours. The dry bone sections were imbedded in EpoThin Epoxy resin (Buehler, Lake

Bluff, USA) and placed in a vacuum chamber (Buehler, Lake Bluff, USA) to remove any air bubbles and then left to cure for a minimum of 24 hours before being sectioned again.

An initial cut was made at the distal portion of the bone section that corresponded to the bottom portion of the ROI which was then ground on an automatic grinder (Buehler, Lake Bluff, USA) using 400 and 600 grit sandpaper. To maintain an even surface, the imbedded thin section was rotated 180 degrees on the grinder every minute until the desired thickness was achieved. Sections were micropolished to remove any grinding imperfections and scars and finally rinsed with distilled water to remove any particles off the surface. The resin 'puck' was then mounted onto a clean micro slide using a small amount of epoxy resin and left to cure for a minimum of 24 hours. The second cut was made at the proximal portion of the section that corresponded to the top portion of the ROI, which was then ground down to a 100 µm thick section using the same grinding procedure previously described.

Thin sections were viewed at 10X magnification using an Olympus BX51 microscope with an Olympus DP72 camera. Images of the thin sections that corresponded to the areas used to define the ROIs produced from the quadrant mask macro (ImageJ) were obtained using Olympus STREAM software. This produced comparable ROIs between the micro-CT slices and the histology sections for qualitative comparison. To compare the slices and sections, sections were visually matched to the corresponding micro-CT slices with the knowledge that each thin section measured 100 µm in thickness which is equivalent to 25 micro-CT slices.

FIGURE 3.1 Images of quadrant mask application

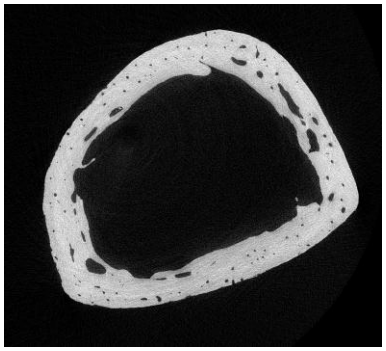

A. micro-CT slice of human MT

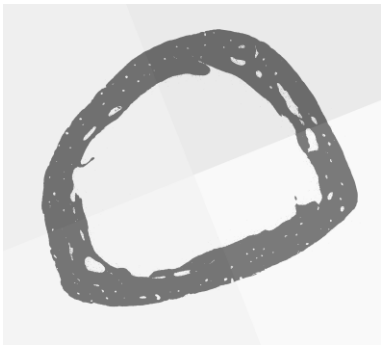

B. Image of human MT micro CT scan after quadrant mask macro (ImageJ) application.

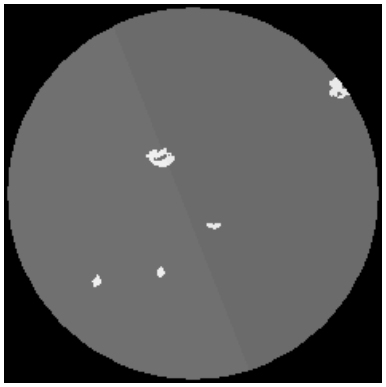

C. Image of ROI extracted from quadrant mask macro (ImageJ).

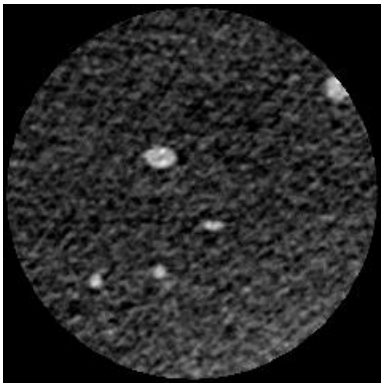

D. Image of a single slice of the ROI.

4: RESULTS

4.1 Statistical procedure

The first order in statistical analysis is deciding which category of tests, parametric or nonparametric, best suit the data set. Motulsky (2010: 179) notes deciding which category to use is particularly important for small sample sizes as to avoid making Type II errors (i.e. rejecting a false null hypothesis) and thus increasing the power of the test. When dealing with small samples, parametric and nonparametric tests can be both advantageous and disadvantageous and these factors should be considered when choosing statistical tests. For example, parametric tests require data to be normally distributed, but with small sample sets, power to test for normality is problematic (Motulsky, 2010: 179). Nonparametric tests do not require data to come from a normal distribution, but Motulsky (2010: 179) notes that nonparametric tests also have very low power when it comes to analyzing small data sets.

For this particular research parametric tests were chosen for analysis based on a few factors. First, if data are indeed normally distributed, nonparametric tests have much less power than their corresponding parametric tests, and in order to obtain comparative levels of power, they actually would require larger sample sizes; this is asymptotic relative efficiency (Motulsky, 2010: 348). The reasoning as to why nonparametric tests have less power than their parametric counterparts is in how the data is analyzed. Nonparametric tests "rank" data and test information of those particular ranks; therefore some data is in essence discarded, whereas parametric tests use all available data for analysis (Hassard, 1991: 276). Sample characteristics such as age, sex and variability were difficult to control for due to the nature of the specimens utilized. Small sample

sizes were also a result of the specimens utilized. Small sample size, as previously noted, can be problematic in detecting normality, yet the data were still found to be normally distributed. Parametric tests may seem unrealistic in terms of the assumptions they require and if these assumptions can be truly met but as noted by Hassard (1991: 277):

> "Second, the parametric tests have been repeatedly shown to be robust to departures from their basic assumptions. In other words, even when there are moderate departures from normality or equality of variance, the parametric tests give reliable results with α and β errors very close to those expected under ideal conditions. This means that the parametric methods can be used with confidence in most practical research situations."

For these various aforementioned reasons, parametric tests were chosen for analysis.

All statistical analysis was performed with SPSS 19.0 (IBM SPSS Statistics 19.0). Due to the small sample size, one sample Kolmogorov-Smirnov (K-S) tests were performed on the averages of the ROIs for each 2D (Appendix, Table 4.1) and 3D (Appendix, Table 4.2) cortical parameter per MC/MT to test for normality. The K-S test showed all the data to be normally distributed.

To test the hypothesis that species, element and the pooled ROIs (independent variables) have a significant effect on Ca.V/TV, Ca.N, Ca.Dm, and MMI (dependent variables), independent t-tests (comparisons between species) and paired t-tests (comparisons within species) was performed at a significance of $p \leq 0.05$. For both significant and non-significant results, r^2 values were also calculated to assess the fraction of variance present between the variables compared (Motulsky, 2010: 247). Levene's test was also employed to assess the homogeneity of variance.

Specifically, t-tests were used to identify potential significant differences among the averages of the cortical parameters measured based on two main categories: 1)

between species; comparing between bears and humans and 2) within species; comparing within humans and within bears. The variables element and method of analysis (2D versus 3D) were also analyzed with t-tests to identify if either would have a significant effect on the cortical parameters measured. For between species, independent t-tests were performed using the averages of the ROIs measured to compare Ca.V/TV, Ca.N and Ca.Dm by species, element and method (2D versus 3D). Between species analysis was further investigated by comparing the averages of the ROIs measured in 2D for both MCs and MTs between bears and humans, as well as for humans and bears between MCs and MTs. The 3D counterpart of these measures was investigated in the same manner, comparing the averages of the ROIs measured in 3D for both MCs and MTs between humans and bears, as well as for humans and bears between MCs and MTs. It should be noted that for MMI, only a 2D measurement is provided as this parameter is only measured in 2D. Also, the MMI for each individual bear and human was calculated based on an entire cross-section, thus statistical testing was derived from one overall measure per bone. For within species analysis, paired t-tests were used to compare the cortical parameters by element and method to identify whether the MCs and MTs within a species would differ.

To test the two methods of analysis utilized in this study, 2D versus 3D, Pearson's Correlation coefficient was used to determine if 2D and 3D measures for each cortical parameter were correlated (see Table 4.15 and Figure 4.7). A correlation coefficient merely indicates if two variables are associated with one another and, if so, how strong that association is. Correlation coefficients do not indicate if two variables are in agreement with one another (Altman-Bland, 1983). To measure agreement between the

2D and 3D measures for Ca.V/TV, Ca.N and Ca.Dm, Bland-Altman plots were computed. Essentially, Altman-Bland tests plot the means against the difference between the means of two variables to determine if variation between the variables changes with the magnitude of the measurements (Altman-Bland, 1983: 311). Paired sample t-tests were then carried out on the Altman-Bland data to interpret whether agreement between the two methods' means was significantly different from zero.

4.2 Quantitative results - statistics

4.2.1 Between-Species t-tests

To test the hypothesis that Ca.V/TV, Ca.N and Ca.Dm are significantly different between human and bear MCs and MTs, the averages of the ROIs of each cortical parameter, stratified by species, element and methodology (2D versus 3D) were examined using independent t-tests ($p \leq 0.05$) (see Tables 4.3 and 4.4 (Appendix); see also Figures 4.1 and 4.2). Independent t-test results of the stratified sample showed a significant difference for the 3D measure of Ca.N between the MCs and MTs of humans and bears. On average, the MCs between humans ($9.68 mm^{-1}$ +/-1.00189) and bears ($5.01 mm^{-1}$ +/-.67518) showed a significant difference $t(8)=3.862$, $p=.005$ with a moderate effect size ($r^2=65.1\%$). The MTs between humans ($4.41\ mm^{-1}$ +/-.54440) and bears ($10.96\ mm^{-1}$ +/-1.10239) also showed a significant difference $t(8)=5.325$, $p=.001$ with a large effect size ($r^2=78.0\%$).

For Ca.Dm, 2D measures of the MCs between humans (17.08 µm +/-2.97899) and bears (8.32 µm +/-1.51737) were significantly different $t(8)=-2.620$, $p=.031$ with a moderate effect size ($r^2=68.0\%$). The metatarsals for 2D Ca.Dm between humans (26.68

μm +/-4.92416) and bears (10.78 μm +/-3.19897) were also found to be statistically significant t(8)=-2.708, p=.027 with a moderate effect size (r^2=70.1%).

For the measure of MMI, the MCs between humans (280.1382000 mm +/-21.38189286) and bears (788.2767000 mm +/-100.66373747) was significant

TABLE 4.3 Independent t-test results for stratified sample – Group statistics

	Units	Species	N	Mean	Std. Deviation	Std. Error Mean	p
2D Ca.V/TV MC	%	bear	5	12.7511	5.95171	2.66169	.113
		human	5	7.2255	3.57640	1.59942	
2D Ca.V/TV MT	%	bear	5	10.3636	5.50876	2.46359	.865
		human	5	9.7798	5.01429	2.24246	
3D Ca.V/TV MC	%	bear	5	12.0199	5.90319	2.63999	.141
		human	5	7.0116	3.47523	1.55417	
3D Ca.V/TV MT	%	bear	5	8.8570	4.09027	1.82922	.788
		human	5	9.6630	5.01518	2.24286	
2D Ca.N MC	#	bear	5	11.7550	12.17439	5.44455	.817
		human	5	13.4200	9.73946	4.35562	
2D Ca.N MT	#	bear	5	9.4200	9.25818	4.14038	.310
		human	5	14.4400	4.62245	2.06722	
3D Ca.N MC	mm^{-1}	bear	5	9.6803	1.50975	.67518	.005*
		human	5	5.0143	2.24030	1.00189	
3D Ca.N MT	mm^{-1}	bear	5	10.9610	2.46503	1.10239	.001*
		human	5	4.4140	1.21732	.54440	
2D Ca.Dm MC	μm	bear	5	8.3200	3.39293	1.51737	.031*
		human	5	17.0800	6.66123	2.97899	
2D Ca.Dm MT	μm	bear	5	10.7800	7.15311	3.19897	.027*
		human	5	26.6800	11.01077	4.92416	
3D Ca.Dm MC	μm	bear	5	87.7350	77.05910	34.46188	.401
		human	5	54.7300	31.46384	14.07106	
3D Ca.Dm MT	μm	bear	5	63.0750	46.94355	20.99379	.942
		human	5	61.2850	25.60785	11.45218	
2D MMI MC	mm	bear	5	788.276700	255.090959	100.663737	.000*
		human	5	280.138200	47.8113659	21.3818928	
2D MMI MT	mm	bear	5	734.957786	147.211676	65.8350629	.001*
		human	5	233.189860	56.3391493	25.1956335	

Abbreviations: Ca.V/TV=cortical porosity; Ca.N=canal number; Ca.Dm=canal diameter; MMI=polar moment of inertia; MC=metacarpal; MT=metatarsal; 2D=two-dimensional; 3D=three-dimensional.
*These abbreviations are used for all subsequent analysis.

t(4.360)=4.938, p=.006 with a large effect size (r^2=84.8%) as well as the MTs between humans (233.1898660 mm +/-25.19563356) and bears (734.9577860 mm +/-65.83506295) at a significance of t(5.147)=7.118, p=.001 and a large effect size (r^2= 90.8%). While no significant results were found for Ca.V/TV, r^2 values for both 2D

(r^2=28.3, p=.113) and 3D (r^2=25.0, p=.141) measures of the MCs between human and bear indicated a medium effect size.

4.2.1.1 2D and 3D Independent t-tests pooled elements between species. Independent t-tests were performed to compare and identify whether the means of independent factors (i.e. species, element, method) analyzed individually would have a significant effect on the cortical parameters measured. The averages of the ROIs for both MCs and MTs measured in 2D (see Tables 4.5, 4.6, Figure 4.3) and 3D (see Tables 4.7, 4.8, Figure 4.4) between bears and humans were used to perform the independent t-tests.

For 2D measures of the combined MCs and MTs between species, independent t-tests revealed MMI as the only significant (t (10.647) =8.148, p=.000) cortical parameter between humans (256.664030 +/-17.4325597) and bears (761.617243 +/-57.3930055) with a moderate effect size (r^2=86.9). For 3D measures of the combined MCs and MTs between species, independent t-tests revealed Ca.N (t (18) =6.631, p=.000) as the only significant cortical parameter between humans (4.7120 mm^{-1} +/-.54641) and bears (10.3220 mm^{-1} +/-.64594).

TABLE 4.5 Group statistics for 2D ROI averages of pooled MCs and MTs between species (bears, humans)

	Species	N	Mean	Std. Deviation	Std. Error Mean
Ca.V/TV	bear	10	11.557	5.5511	1.7554
	human	10	8.503	4.3211	1.3664
Ca.N	bear	10	10.590	10.2706	3.2479
	human	10	13.931	7.2068	2.2790
Ca.Dm	bear	10	14.000	10.7497	3.3993
	human	10	22.000	11.3529	3.5901
MMI	bear	10	761.617243	181.4926193	57.3930055
	human	10	256.664030	55.1265941	17.4325597

Figure 4.1 Bar graphs representing the means of the pooled MC and MT ROIs for each 2D cortical parameter compared against the factor species. Error bars represent the 95% confidence interval.

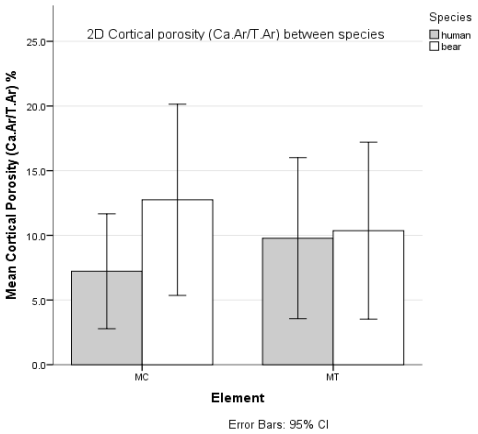

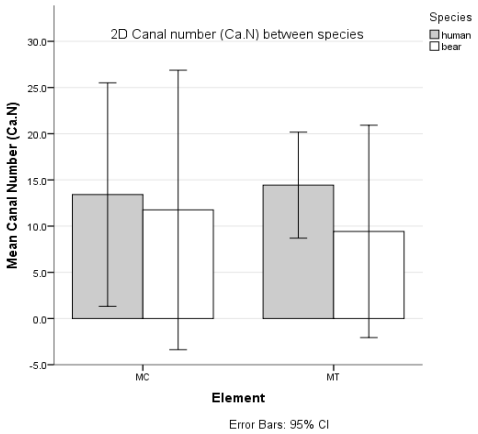

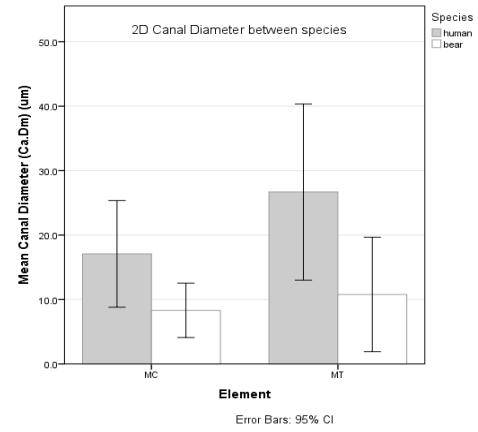

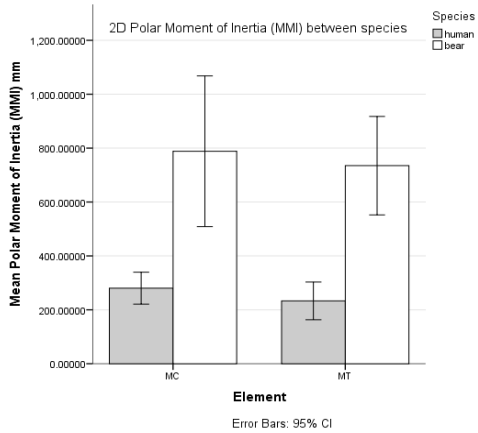

Figure 4.2 Bar graphs representing the means of the pooled MC and MT ROIs for each 3D cortical parameter compared against the factor species. Error bars represent the 95% confidence interval.

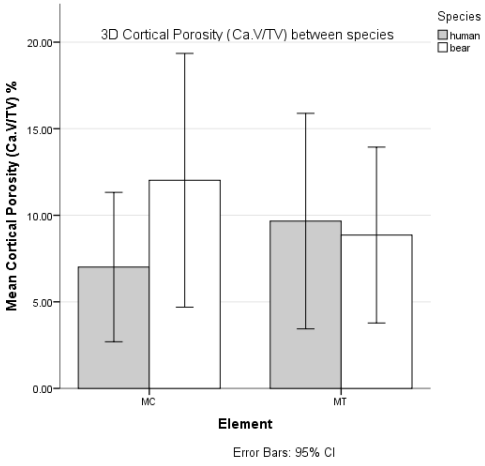

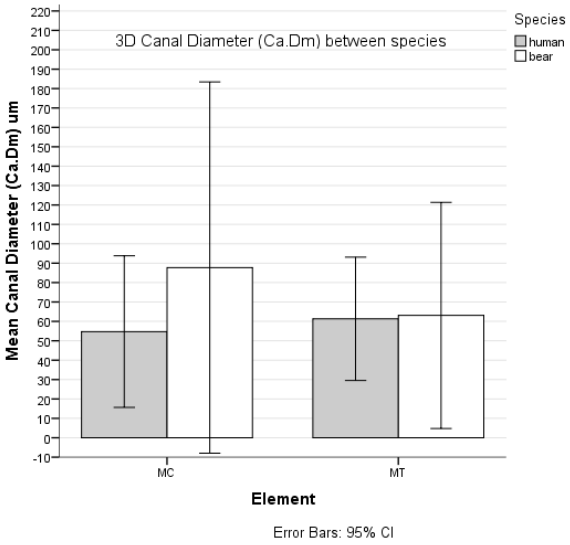

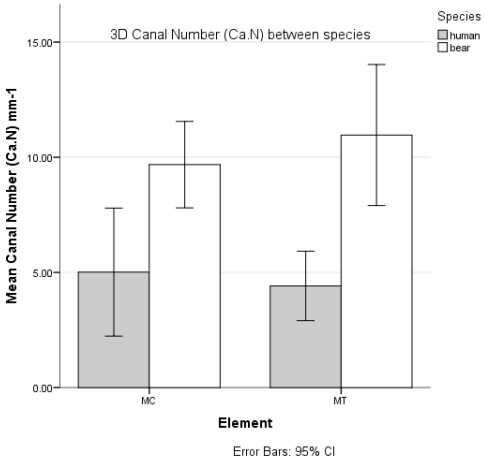

TABLE 4.6 Independent t-test results 2D ROI averages of pooled MCs and MTs between species (bears, humans)

Parameter	Levene's statistic F	Sig.	t	df	Sig. (2-tailed)	Mean Difference	r2
Ca.V/TV	1.199	.288	1.373	18	.187	3.0547	9.6
Ca.N	.867	.364	-.842	18	.411	-3.3410	3.6
Ca.Dm	.013	.910	-1.618	18	.123	-.0080000	13.0
MMI	10.676	.004	8.418	10.647	.000	504.9532130	86.9

TABLE 4.7 Group statistics for 3D ROI averages of pooled MCs and MTs between species (bears, humans)

	Species	N	Mean	Std. Deviation	Std. Error Mean
Ca.V/TV	bear	10	10.4385	5.06976	1.60320
	human	10	8.3373	4.30105	1.36011
Ca.N	bear	10	10.3220	2.04266	.64594
	human	10	4.7120	1.72790	.54641
Ca.Dm	bear	10	75.4070	61.54176	19.46121
	human	10	58.0090	27.26498	8.62195

TABLE 4.8 Independent t-test results 3D ROI averages of pooled MCs and MTs between species (bears, humans)

Parameter	Levene's statistic F	Sig.	t	df	Sig. (2-tailed)	Mean Difference	r2
Ca.V/TV	.848	.369	.999	18	.331	2.10115	5.3
Ca.N	.157	.697	6.631	18	.000*	5.61000	70.6
Ca.Dm	6.117	.024	.817	12.402	.429	17.39800	5.3

4.2.1.2 2D and 3D Independent t-tests within species, between elements. Average 2D ROI values for humans and bears between element (see Table 4.9, 4.10; Figure 4.5) and average 3D ROI values for humans and bears between element (see Table 4.11, 4.12; Figure 4.6) were analyzed to determine whether element would have a significant effect on the combined values of species for all the cortical parameters analyzed. Independent t-tests showed that in either 2D or 3D, no cortical parameters were statistically significant and all r^2 values displayed small effect sizes.

TABLE 4.9 Group statistics for 2D ROI averages of pooled bears and humans between element (MCs, MTs)

	Element	N	Mean	Std. Deviation	Std. Error Mean
Ca.V/TV	MC	10	9.988	5.4689	1.7294
	MT	10	10.072	4.9756	1.5734
Ca.N	MC	10	12.588	10.4319	3.2989
	MT	10	11.933	7.3865	2.3358
Ca.Dm	MC	10	16.000	9.6609	3.0551
	MT	10	20.000	13.3333	4.2164
MMI	MC	10	534.207450	308.6384626	97.6000515

TABLE 4.10 Independent t-test results 2D ROI averages of pooled bears and humans between element (MCs, MTs)

Parameter	Levene's statistic		t	df	Sig.	Mean	r2
	F	Sig.			(2-tailed)	Difference	
Ca.V/TV	.121	.732	-.036	18	.972	-.0834	.008
Ca.N	.403	.533	.162	18	.873	.6550	.2
Ca.Dm	.045	.834	-.768	18	.452	-.0040000	.04
MMI	.003	.957	.378	18	.710	50.1336270	0.8

TABLE 4.11 Group statistics for 3D ROI averages of pooled bears and humans between element (MCs, MTs)

	Element	N	Mean	Std. Deviation	Std. Error Mean
Ca.V/TV	MC	10	9.5158	5.27476	1.66802
	MT	10	9.2600	4.33530	1.37094
Ca.N	MC	10	7.3460	3.04888	.96414
	MT	10	7.6880	3.90921	1.23620
Ca.Dm	MC	10	71.2340	58.15233	18.38938
	MT	10	62.1820	35.66110	11.27703

TABLE 4.12 Independent t-test results 3D ROI averages of bears and humans between element (MCs; MTs)

Parameter	Levene's statistic		t	df	Sig.	Mean	r2
	F	Sig.			(2-tailed)	Difference	
Ca.V/TV	.419	.525	.118	18	.907	.25597	.1
Ca.N	1.293	.270	-.218	18	.830	-.34200	1.0
Ca.Dm	.947	.343	.420	18	.680	9.05200	1.0

Figure 4.3 Bar graphs representing the 2D pooled ROI measures between species. Error bars represent the 95% confidence interval.

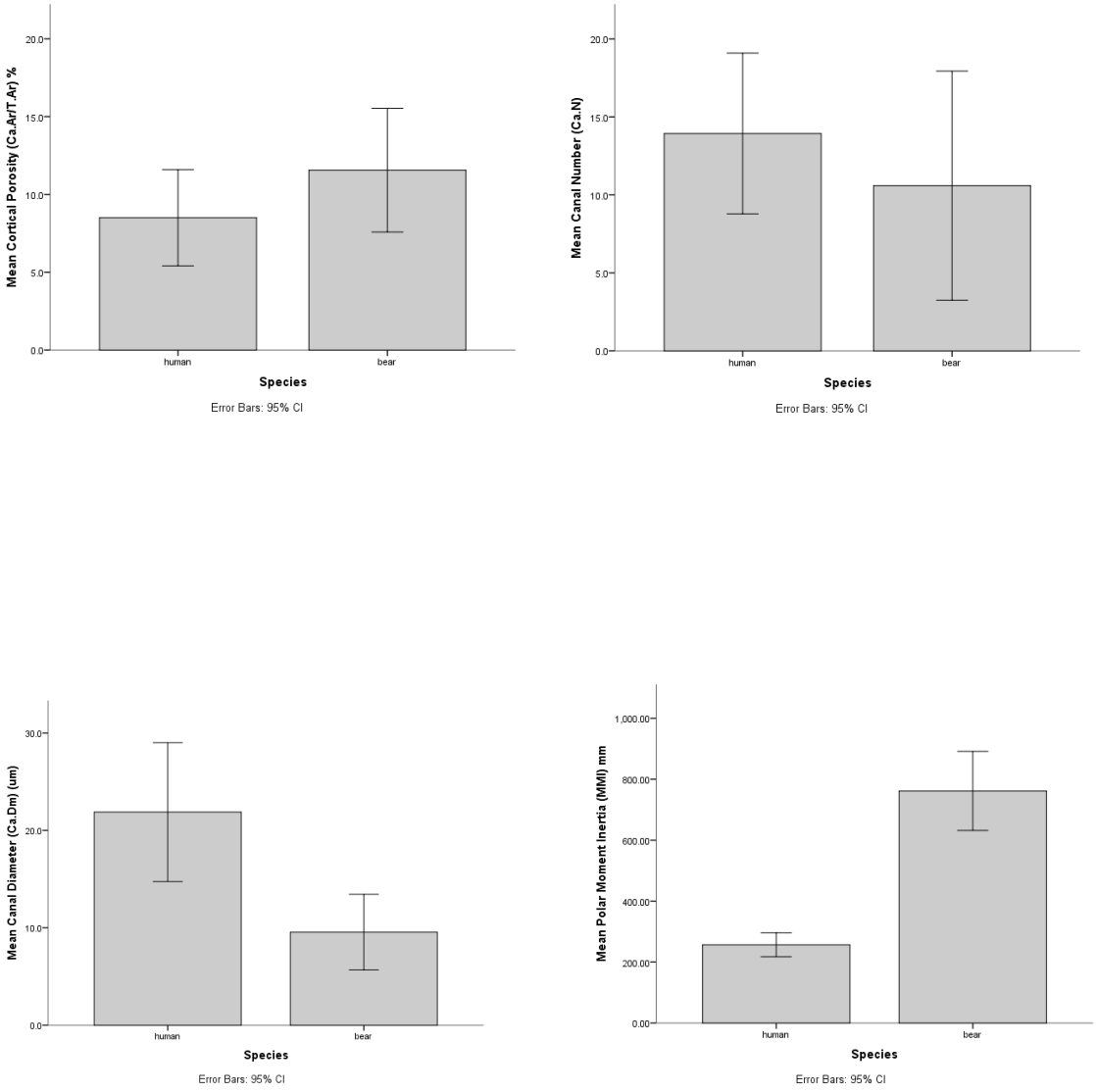

Figure 4.4 Bar graphs representing the 3D pooled ROI measures between species. Error bars represent the 95% confidence interval.

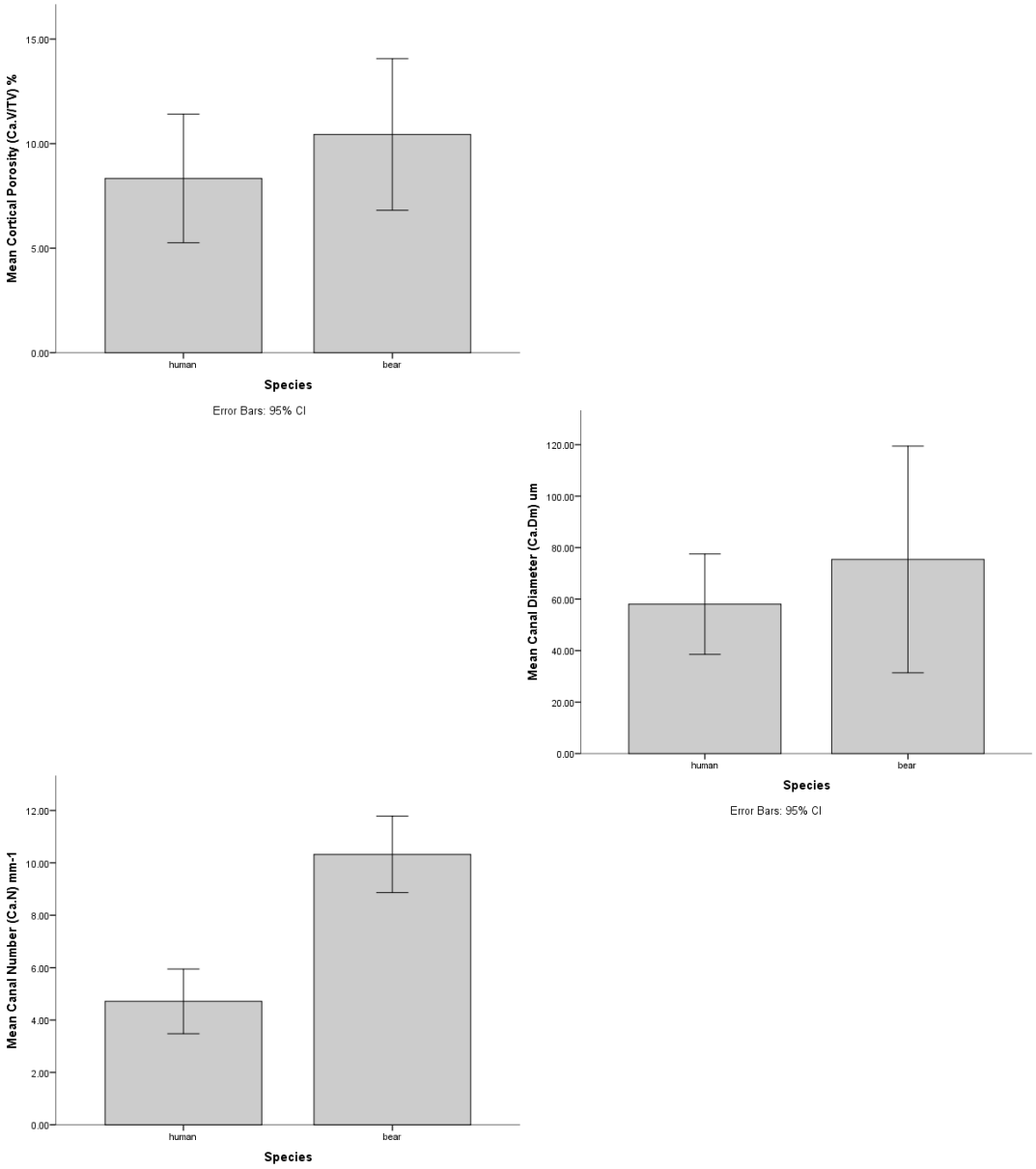

4.2.2 Within-Species t-tests

To test the hypothesis that the MCs and MTs among bear paws are similar to one another, whereas the MCs and MTs between human hands are different, paired t-tests were carried out for both the human sample as well as the bear sample, and the level of significance was set as $p<0.05$. Paired t-tests compared the 2D and 3D averaged ROI measures of the MCs and MTs for each measured cortical parameter within the bear sample set (see Tables 4.13) and within the human sample set (see Tables 4.14).

TABLE 4.13 Bear paired samples statistics

	Parameter	Mean	N	Std. Deviation	Std. Error Mean	Sig. (2-tailed)	r^2
Pair 1	2D Ca.V/TV MC	12.7511	5	5.95171	2.66169		
	2D Ca.V/TV MT	10.3636	5	5.50876	2.46359	.419	16.8
Pair 2	3D Ca.V/TV MC	12.0199	5	5.90319	2.63999		
	3D Ca.V/TV MT	8.8570	5	4.09027	1.82922	.200	37.2
Pair 3	2D Ca.N MC	11.7550	5	12.17439	5.44455		
	2D Ca.N MT	9.4200	5	9.25818	4.14038	.271	29.2
Pair 4	3D Ca.N MC	9.6803	5	1.50975	.67518		
	3D Ca.N MT	10.9610	5	2.46503	1.10239	.261	30.3
Pair 5	2D Ca.Dm MC	.0148	5	13.23	5.92		
	2D Ca.Dm MC	.0108	5	7.13	3.19	.445	15.2
Pair 6	3D Ca.Dm MC	87.7350	5	77.05910	34.46188		
	3D Ca.Dm MT	63.0750	5	46.94355	20.99379	.464	14.4

TABLE 4.14 Human paired samples statistics

	Parameter	Mean	N	Std. Deviation	Std. Error Mean	Sig. (2-tailed)	r2
Pair 1	2D Ca.V/TV MC	7.2255	5	3.57640	1.59942		
	2D Ca.V/TV MT	9.7798	5	5.01429	2.24246	.346	25.0
Pair 2	3D Ca.V/TV MC	7.0116	5	3.47523	1.55417		
	3D Ca.V/TV MT	9.6630	5	5.01518	2.24286	.330	25.0
Pair 3	2D Ca.N MC	13.4200	5	9.73946	4.35562		
	2D Ca.N MT	14.4400	5	4.62245	2.06722	.836	1.2
Pair 4	3D Ca.N MC	5.0143	5	2.24030	1.00189		
	3D Ca.N MT	4.4140	5	1.21732	.54440	.460	16.0
Pair 5	2D Ca.Dm MC	.0162	5	5.57	2.49		
	2D Ca.Dm MT	.0266	5	10.96	4.90	.120	49.0
Pair 6	3D Ca.Dm MC	54.7300	5	31.46384	14.07106		
	3D Ca.Dm MT	61.2850	5	25.60785	11.45218	.761	4.0

Figure 4.5 Bar graphs representing the 2D pooled ROI measures between element. Error bars represent the 95% confidence interval.

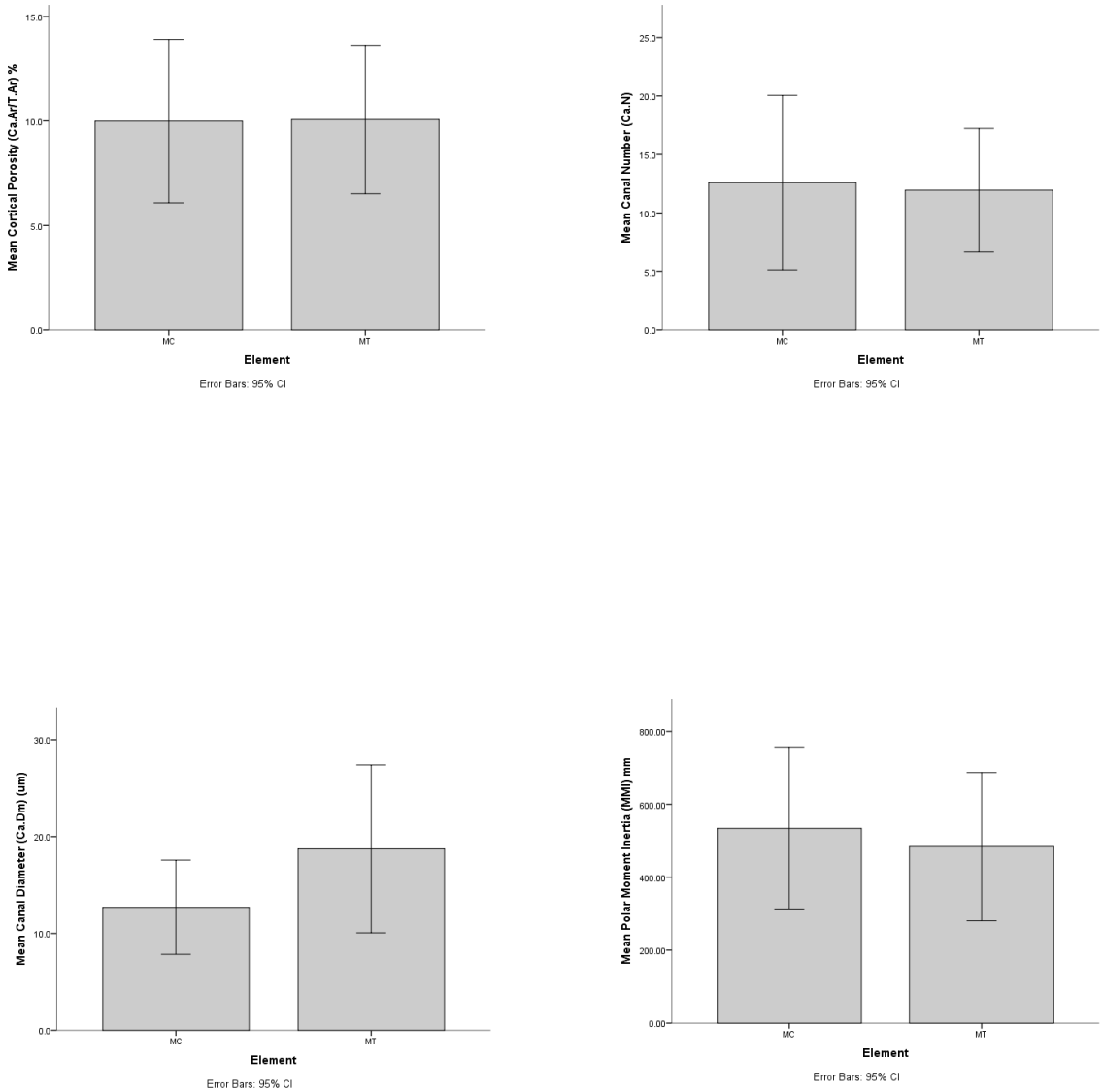

Figure 4.6 Bar graphs representing the 3D pooled ROI measures between element. Error bars represent the 95% confidence interval.

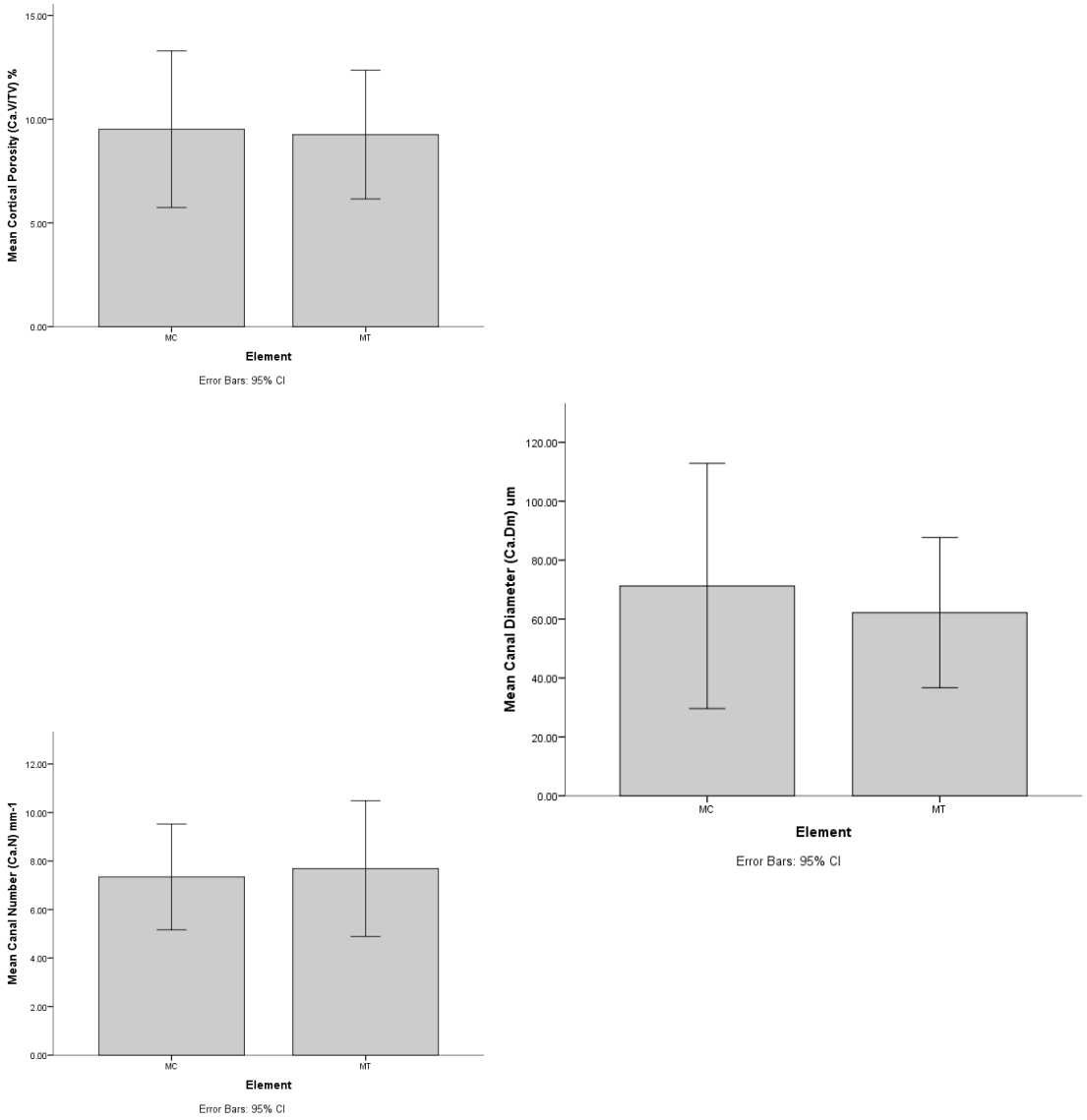

Paired t-tests revealed no significance difference between the paired cortical parameters for either the human or bear sample set. Although no significant differences were found, r^2 values within the human sample for pairs 1, 2 and 5 did show medium effect sizes (25.0, 25.0 and 49.0) respectively.

4.2.3 Comparison of methodology, 2D versus 3D

Pearson coefficient correlation scatterplots (see Figure 4.7) reveal for cortical porosity, the points lie very close to the line of identity with a strong and significant, positive correlation between the 2D and 3D measures, $r=0.967$, $p<0.000$. Unlike cortical porosity, plots for canal number ($r=-.357$, $p<0.123$) and canal diameter ($r=0.199$, $p<0.400$) show a deviation away from the line of identity. Table 4.15 presents the average of the measures and the difference of the average measures of which the Bland-Altman plots (see Figure 4.7) were calculated. The plot for cortical porosity shows a non-significant ($p>0.081$) agreement between the 2D and 3D measures. Bias is very small, (0.64%) and in general, there is not a distinct directional trend evident among the difference of the mean and the average measures, indicating that one method is neither over or underestimating the measure of cortical porosity over the other.

For canal number, the Bland-Altman plots clearly show that the 2D and 3D measures do not agree and in fact are measuring the canals differently. Bias is small (4.74%), but significant ($p<0.001$); 2D seems to overestimate canal populations over 3D measures. In general, as the difference between the mean increases, so to does the average measure. Variability is also consistent, the scatter around the line of bias increases as the average measure increases.

TABLE 4.15 Statistics for the means and the differences of the means for all 2D and 3D measurements

Individual	Ca.V/TV Ave	Ca.V/TV Diff	Ca.N Ave	Ca.N Diff	Ca.Dm Ave	Ca.Dm Diff
1	19.15	.66	7.96	-.71	113.95	-206.30
2	17.31	.90	7.23	-3.16	63.35	-75.90
3	8.43	1.07	8.46	-7.52	24.94	-28.68
4	4.98	.45	8.47	-2.14	25.67	-22.95
5	12.06	.58	21.48	23.91	33.03	-21.65
6	7.14	.30	9.41	3.79	34.62	-19.63
7	9.13	.30	8.96	4.09	47.16	-23.12
8	11.36	.31	5.51	.78	77.94	-55.88
9	5.98	.08	16.49	27.81	42.97	.47
10	1.98	.08	5.72	5.57	19.55	-4.70
11	11.45	.61	7.52	-5.48	72.57	-75.53
12	9.21	1.02	10.83	-4.29	23.40	-23.60
13	6.94	.97	9.23	-9.20	18.09	-16.58
14	3.91	.40	6.76	-6.65	18.77	-13.13
15	16.55	4.52	16.64	17.92	78.78	-78.75
16	10.16	.18	12.51	13.59	48.89	-13.38
17	18.15	.10	9.49	10.79	97.55	-14.30
18	5.64	.13	10.89	10.82	35.52	-5.03
19	8.14	.07	8.81	12.18	50.89	4.63
20	6.54	.09	5.45	2.77	53.78	-11.55

Abbreviations: Ave (average); Diff (difference).

Finally, for canal diameter, the 2D and 3D measures do not agree. A significant ($p<0.001$) negative bias indicates that 35% of the time, 2D underestimates canal diameter. The average of measures tend to slightly increase as the difference increases until around 60um when the difference between the mean sharply drop as average increase. The variability of the scatter is also tends to deviate from the line of identity as the average measure increases.

4.3 Qualitative results

4.3.1 Visual comparison of histology ROIs to Micro-CT ROIs

Qualitative assessment of the 2D histology sections against the 3D Micro-CT slices was performed to validate the approach of using Micro-CT to assess microscopic cortical bone. Corresponding ROIs for the Micro-CT slices and the histology thin sections were identified (see Figure 4.8). Matches between the slices and sections for the

Figure 4.7 Pearson correlation Scatterplots (left) and Bland-Altman plots (right) for cortical porosity, canal number and canal diameter measured in 2D and 3D. Line of identity is shown for the Pearson correlation scatterplots and 95% lines of limit shown for the Bland-Altman plots.

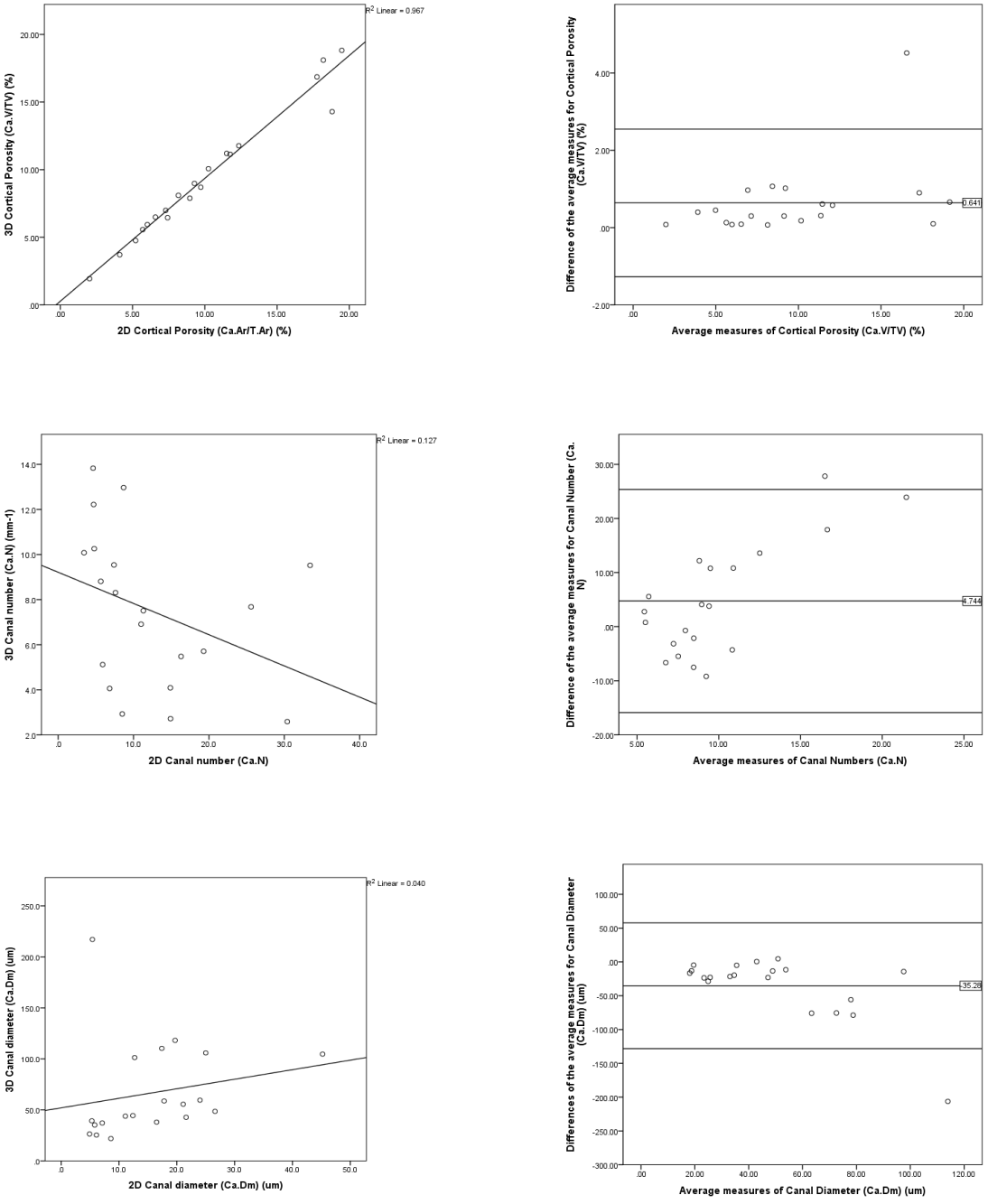

bear samples were more difficult to identify compared to the human sample. Bear cortical canals were found overall to be smaller in diameter (M=.01279mm) compared to those of humans (M=.021445mm). This was also evident during Micro-CT analysis because the bear canals proved difficult to visualize and required the maximum level of filtering to aid in bone contrast.

4.3.2 Visual analysis of microscopic structures - histology

Qualitative analysis also included observation of the superior, inferior, medial and lateral regions of two paired human and two paired bear histology sections both within and between humans and bears. These observations served as a visualization of the statistical results, but also as a means to highlight any underlying trends or patterns not statistically recognized as a result of sample size. Histology sections were visually inspected to identify general osteon shape and canal size, because relatively round osteons are noted as indicators of the biomechanical forces exerted upon bone (Stout, 2003: 240). Other bone characteristics such as bone type (primary and/or secondary), bone resorption activity, and when possible, canal orientation were also inspected (see Figures 4.10, 4.11, 4.12 and 4.13).

Figure 4.8 2D Histology sections matched to corresponding 3D Micro-CT slices. Image A represents bear SUO900436's MT superior ROI (histology section) compared to its corresponding superior ROI of Image B (Micro-CT slice). Image C represents human PA-4-16's MT lateral ROI (histology section) compared to its corresponding lateral ROI of Image D (Micro-CT slice).

Image A

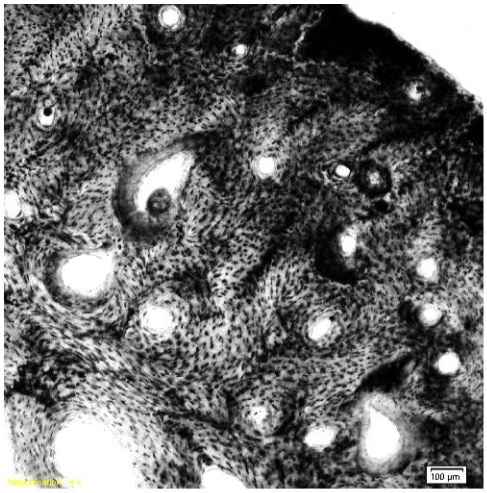

Image B

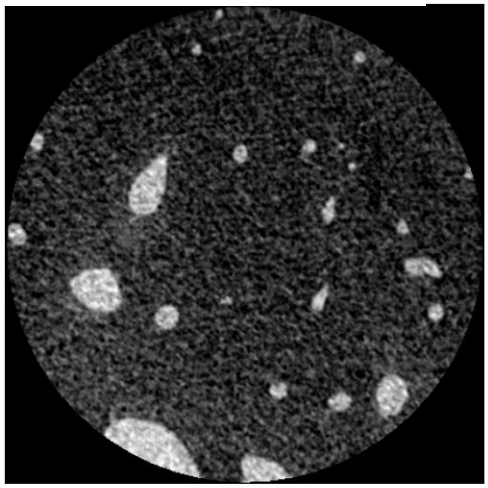

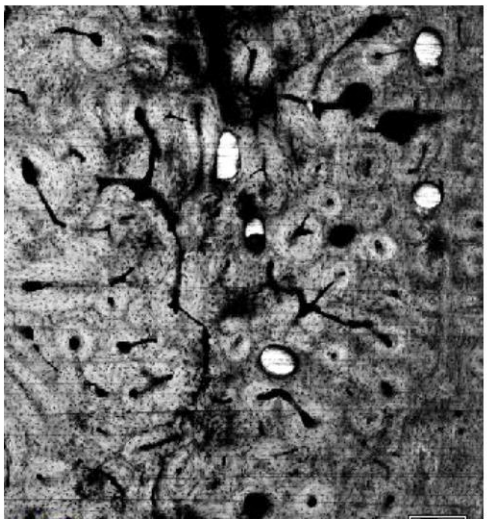

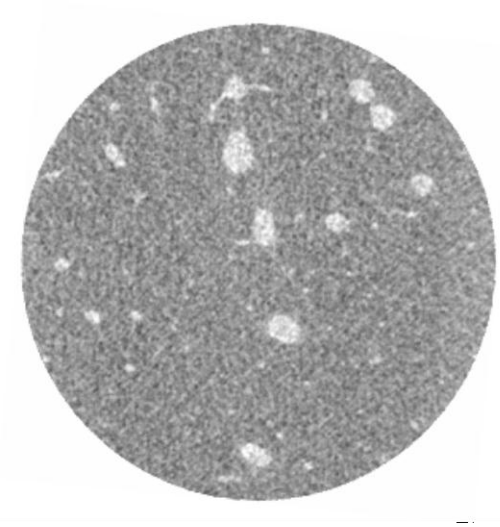

Image C

Image D

4.3.2.1 Superior region. Comparison of the superior region among human MCs and MTs revealed primary and secondary bone present in both MCs and MTs. Resorption spaces appeared to be higher in the MCs; however, one interesting observation in the MTs was the presence of what seems to be osteon banding (see Figure 4.9). According to Mulhern and Ubelaker (2001), osteon banding can be used to differentiate between human and nonhuman bone as osteon bands are more characteristic of nonhuman bone. In 60 human histology sections analyzed, only two bone sections displayed osteon bands, however even then they were not defined in a distinct row (Mulhern and Ubelaker, 2001). Osteons were more numerous among the MCs; however, canal diameters were relatively large in size in both elements. Osteon shape was mainly circular, but a small portion of elliptical shaped osteons was observed.

Comparison of the superior region among bear MCs and MTs revealed bone type as mainly secondary, but primary bone was evident in one of the MCs observed. Similar to the human superior regions, resorption spaces were prominent in the MCs and osteons were mainly circular in appearance. Unlike the human superior regions, osteon populations were numerous in both the MCs and MTs, whereas canal diameters of the MCs were smaller than those observed in the MTs. Radial canals were also clearly observed in both MCs and MTs.

4.3.2.2 Inferior region. Comparison of the inferior region for the human sections showed secondary bone as the main type of bone present for both MCs and MTs, however primary bone was also evident in both element types. While resorption spaces we

Figure 4.9 Example of osteon banding in human MC (A, B) and bear MCs (C, D). Arrows point to bands.

Image A: Human PA-4-16 MC

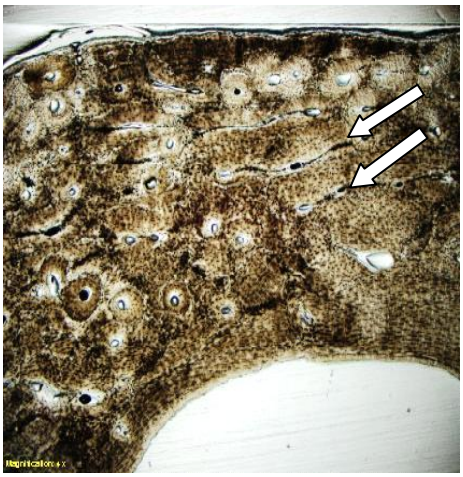

Image B: Human PA-4-16

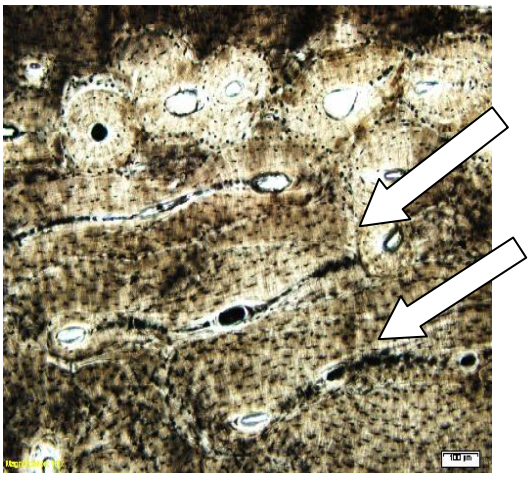

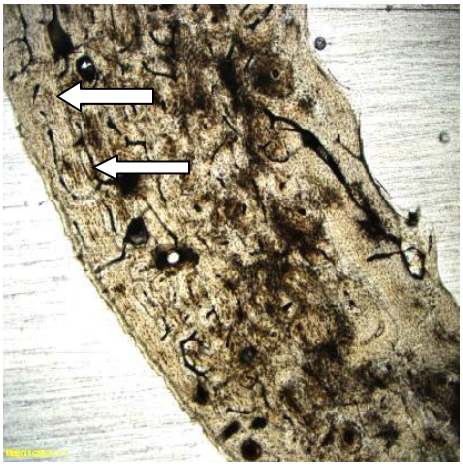

Image C: Bear SUO900436 MC Inferior

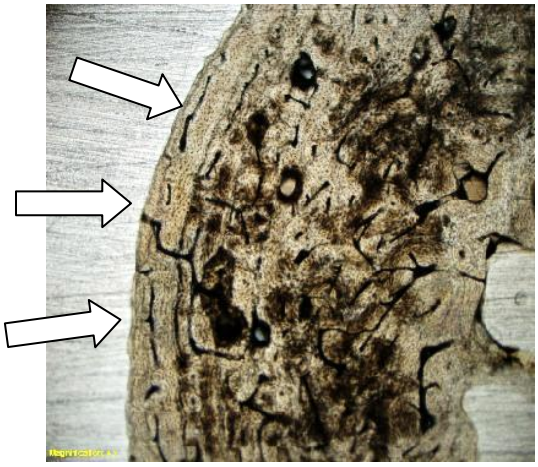

Image D: Bear SUO900436 MC Medial

present in both MCs and MTs, much higher amounts were observed in the MTs. Osteons were much more numerous in the MCs, and minimal numbers were observed in the MTs. Metacarpal canal diameters were smaller than the MTs. Round osteons were present in both MCs and MTs.

Comparison of the bear inferior regions displayed mainly secondary bone patterns, although some primary bone was also observed in the MCs. Resorption spaces were more prominent in the MTs compared to the MCs. Osteon populations were abundant for both MCs and MTs. Canal diameter size ranged from small to moderate in both elements, but large canals were also observed in the MTs. Both MCs and MTs displayed circular osteons. Radial canals were also present and osteon banding was noted in the MCs.

4.3.2.3 Lateral region. Human lateral regions showed similar bone patterns, both primary and secondary bone was present in the MCs and MTs. In general, resorption spaces were high throughout the lateral regions of the MCs and MTs. Osteon populations in the MCs were very high, whereas they were only moderate in the MTs. Canal diameters were smaller in the MCs. Interestingly, a higher number of elliptical osteons were noted in the lateral regions compared to the superior and inferior regions.

Bear lateral bone regions displayed similar bone patterns between the MCs and MTs, mainly secondary bone; still primary bone was present in both. Also, resorption spaces were similar and were present in both elements in similar proportions. Osteon populations were high and canal diameters ranged from small to moderate in both MCs and MTs. Circular and elliptical shaped osteons were also present in both MCs and MTs.

Radial canals were very prominent in the MTs, and again, osteon banding was noted in the MCs.

4.3.2.4 Medial region. Finally, comparison of the medial regions for the human MCs and MTs displayed similar bone patterns for each; both primary and secondary bone were present. Resorption spaces were prominent in both MCs and MTs; yet the MTs displayed very high levels of resorption. Osteon populations were very high for both MCs and MTs, and canal diameters ranged in size from moderate to large, with the largest osteons observed in the MTs. Round and elliptical shaped osteons were present in both MCs and MTs.

Medial regions of the MCs and MTs for the bear sections showed primary and secondary bone in both elements. Resorption spaces were also present, although they were less obvious compared to the resorption spaces of the human medial regions. Like the human medial regions, osteon populations were numerous in both MCs and MTs; however canal diameter size were much smaller. Radial canals were prominent in both MCs and MTs, and once again, osteon banding was observed in the MCs.

Figure 4.10 Histology sections displaying microscopic cortical bone structures for human MCs. Images represent superior (A), inferior (B), lateral (C) and medial (D) regions.

Image A: A4 MC Superior

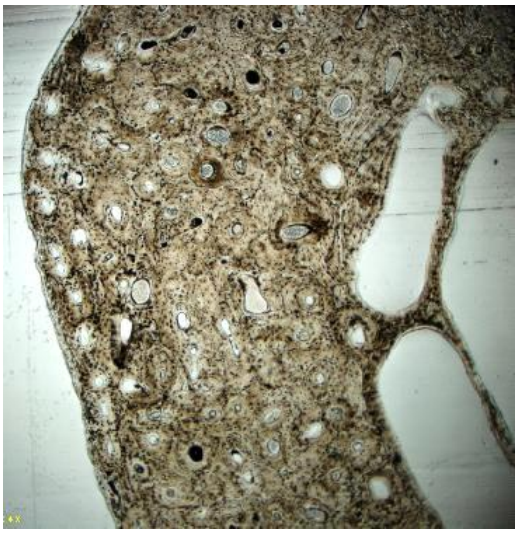

Image B: A4 MC Inferior

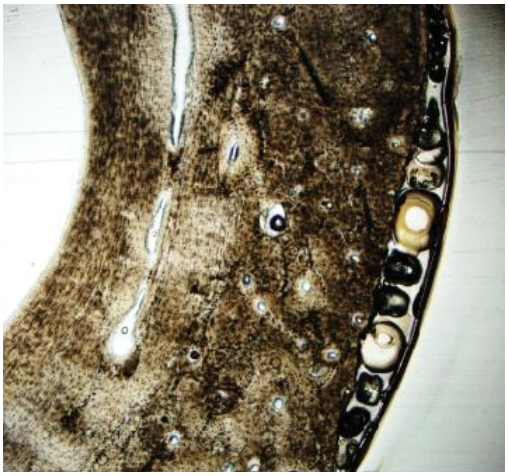

Image C: PA-4-16 MC Lateral

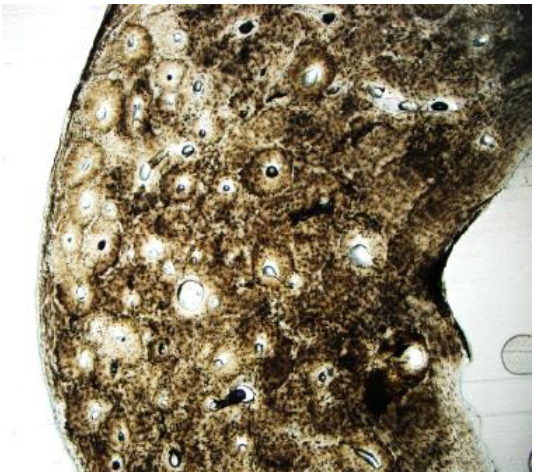

Image D: PA-4-16 MC Medial

Figure 4.11 Histology sections displaying microscopic cortical bone structures for human MTs. Images represent superior (A), inferior (B), lateral (C) and medial (D) regions.

Image A: A4 MT Superior

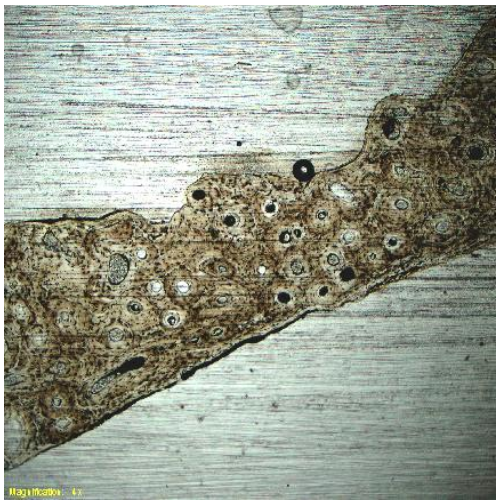

Image B: PA-4-16 MT Inferior

Image C: A4 MT Lateral

Image D: PA-4-16 MT Medial

Figure 4.12 Histology sections displaying microscopic cortical bone structures for bear MCs. Images represent superior (A), inferior (B), lateral (C) and medial (D) regions.

Image A: SUO900802 Superior

Image B: SUO900436 MC Inferior

Image C: SUO900802 Lateral

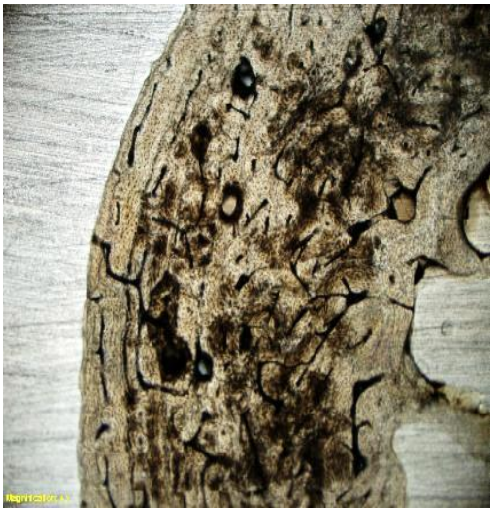

Image D: SUO900436 Medial

Figure 4.13 Histology sections displaying microscopic cortical bone structures for bear MTs. Images represent superior (A), inferior (B), lateral (C) and medial (D) regions.

Image A: SUO900802 MT Superior

Image B: SUO900436 MT Inferior

Image C: SUO900802 MT Lateral

Image D: SUO900436 MT Medial

5: DISCUSSION & CONCLUSIONS

5.1 Discussion

Bone is unique in that it is a complex and dynamic tissue that continually renews itself throughout life and has the ability to respond and adapt to the mechanical demands placed upon it. It has been widely accepted that biomechanical forces greatly influence and/or govern the shape and arrangement of bone (Seeman, 2008; Basillais et al. 2007; Seeman and Delmas, 2006; Chen et al. 2004; Skedros et al. 2004; Skedros et al. 2003; Burr et al. 2002; Turner, 1998; Currey, 1984; Laynon, 1984; Laynon and Baggott, 1976) and in turn, the mode of locomotion an organism exhibits affects the structure and appearance of bone.

Gross skeletal characteristics such as the general shape of bone and bone cross-geometric parameters have been shown to serve as valuable parameters to infer a species mode of locomotion. However, through the comparison of the strikingly similar skeletal elements of black bears and humans, it is argued that a strictly gross morphological analysis may not necessarily provide a comprehensive and accurate assessment of species' modes of locomotion, therefore requiring a microscopic analysis of cortical bone structures. As well, microscopic analysis carried out in 3D using Micro-CT as opposed to traditional 2D histology is proposed as a necessary means of analysis because bone is naturally a 3D structure. Thus, to fully appreciate a bone's characteristics, analysis must be also performed in 3D (Basillais et al., 2007; Stout et al., 1999; Cooper et al., 2003: 169).

Numerous studies have assessed the microscopic anatomy of both trabecular (Muller, 2009; Fajardo et al., 2002; Ruegsegger et al., 1996) and cortical (Muller, 2009;

Basillais et al., 2006; Chen et al., 2004; Jones et al., 2004; Cooper et al., 2011, 2003; Wachter et al., 2002) bone. However, to my knowledge, this study is the first to assess 3D microscopic cortical bone structures, specifically cortical porosity, canal populations, canal diameter, and polar moments of inertia, as biomechanical indicators to infer a species mode of locomotion between the skeletally similar elements of bipedal humans and quadrupedal black bears.

Through the peculiar case of similar skeletal morphology between the third metacarpals and metatarsals of two species, bears and humans, that exhibit different modes of locomotion, it was hypothesized that: 1) cortical microscopic bone structures of human and bear MCs and MTs would differ due to their different modes of locomotion, and within species, human MCs and MTs microscopic structures would differ, whereas bear microscopic MCs and MTs would be similar to one another 2) microscopic bone morphology (as opposed to gross skeletal morphology) in fact provides a more accurate and representative method to infer a species' mode of locomotion, and finally 3) to assess whether these microscopic morphologies can be accurately observed and analyzed non-destructively, through the use of microcomputed tomography imaging (Micro-CT).

5.1.1 Between-species

This study supported the hypothesis that biomechanical loading affected the microscopic structures of cortical bone, as evidenced in the comparative analyses of species and skeletal element. Analysis of the cortical parameters stratified by species, element and methodology demonstrated that in 3D, number of canals significantly differed between the MCs of humans and bears as well as the MTs of humans and bears.

For the 2D measure of canal diameter, similar findings were found; human and bear MCs and human and bear MTs significantly differed from one another.

Similar findings to this study have been reported (Skedros et al., 2003; Su et al., 1999; Schaffler and Burr, 1984). Skedros et al. (2003) suggested higher rates of bone remodeling, and thus Haversian canals located in the distal forelimb bones of Rocky Mountain mule deer, was a reaction to the locomotor biomechanical forces that, in turn, initiated bone remodeling as an adaptive response. Schaffler and Burr (1984) found that the amount of osteonal bone within the mid-diaphysis of primate femora differed due to locomotion patterns, and that the percentage of osteonal bone correlated to the mode of locomotion exhibited, specifically identifying arboreal and terrestrial quadrupedalism and suspensory and bipedalism, suggesting that remodeling is correlated to the means in which bone is habitually loaded.

Su et al. (1999) found artiodactyl calcaneus cortical bone osteon remodeling rates, osteon morphology and mineral content correlated in part with the principal longitudinal compression and tension strains in opposing cranial and caudal cortices, respectively. These studies and the findings of this study support the argument that biomechanical stressors do have an identifiable affect on microscopic bone structure and form, which can subsequently be utilized as indicators of such biomechanical factors.

In the stratified sample, MMI was also found to be statistically significant between the MCs and MTs of humans and bears. Bear bone is naturally more robust than human bone, therefore the significance of MMI between the two species was expected, as the cross-sectional area of bone in bears would be greater than those of humans, implying that the MCs and MTs of bears are stronger and stiffer overall than those of humans.

Bar graphs that provide a visual interpretation of the statistical data and 2D histology sections from two individual humans and two individual bears also point to potential trends between species and element. Statistically, the parameter Ca.V/TV was not found to be significant for either between or within subjects t-tests, however 2D and 3D bar graphs (Figures 4.1 and 4.2) revealed higher levels of porosity overall in the MCs, and more specifically, bear MCs were found to be more porous than human MCs. Cortical porosity is a reflection of bone remodeling and strength and because bears use their MCs for locomotion whereas humans do not, it is not surprising that the bear MCs displayed higher levels of porosity. Furthermore, humans and bears both use their MTs for locomotion, thus is not surprising that the Ca.V/TV measures between human and bear MTs showed little difference between one another. Although cortical porosity was not statistically significant, MMI, which is a measure of strength, was found to be significant between the MCs of humans and bears, supporting the idea that cortical porosity does differ between species.

Qualitative assessment of the histology sections (Figures 4.5 through 4.10) provided evidence that bear and human MC and MT microscopic cortical structures possibly differed due to their different modes of locomotion. Histology sections revealed overall that bear bone has significantly more cortical canals than human bone. This observation agrees with the 3D statistical and bar graph results; however, interestingly, it disagrees with the 2D bar graph that shows humans having slightly higher populations of cortical canals. Histological analysis also revealed that overall, human canal diameters (Ca.Dm) were larger than those of bears, which agrees with the 2D bar graph data, but the 3D imagery shows that bears actually have larger canal diameters. The discrepancy

between the 2D and 3D data for canal diameter could be a result of bear bone being more porous than human bone according to the bar graph data.

The factors species and element were also tested individually to determine if either one had a more significant affect on the microscopic bone structures. Species was clearly having an affect on the cortical parameters analyzed. Bar graph analysis indicates that for each cortical parameter analyzed in both 2D and 3D, humans and bears differed from one another. Visually, the histology sections of the humans and bears revealed a similar pattern, i.e. human and bear bone differed for each cortical parameter observed.

The factor element, in comparison to the factor species, did not seem to have as significant an effect between humans and bears. For example, comparison of the 2D and 3D graphs and histology sections for the parameter Ca.V/TV showed no real differences evident between the MCs and MTs. Canal populations (Ca.N) between the MCs and MTs differed only slightly according to the 2D graph and histology data, whereas in the 3D graph, the MTs showed an insignificantly higher canal population. The same was found for canal diameter; the 2D data indicate the MCs had slightly larger canal diameters, whereas in 3D, canal diameters are slightly larger in the MTs.

5.1.2 Within-species

Comparison of the paired cortical parameters within species found no statistically significant results for either the bear or human sample. Bears exhibit a quadrupedal mode of locomotion, utilizing both their frontlimbs and hindlimbs for locomotion in a similar fashion, thus significant differences between their MCs and MTs were not expected to be displayed which is supported by the paired t-test. Visual inspection of the histology sections also supported the paired t-test results. Canal numbers in both the bear

MCs and MTs were regularly found to be abundant. Canal diameter size was also similar between the MCs and MTs. Resorption spaces were also prominent in both the MCs and MTs; however, one bear's MC showed higher levels of resorption and one bear's MT showed lower levels of resorption.

Surprisingly, the paired cortical parameters for the human sample were not significant when differences were expected due to the fact that humans do not use their hands for locomotion. While differences between human MCs and MTs were not statistically found, r^2 values, bar graph and histology data reveal differences. Calculations of r^2 values for the human pairs 1 (2D Ca.V/TV), 2 (3D Ca.V/TV) and 5 (2D Ca.Narea) showed medium to moderate effect sizes, 25.0, 25.0 and 49.0, respectively. These values indicate that with a larger sample size, these pairs that represent cortical porosity and canal area may actually differ between the MCs and MTs of humans.

Histological analysis of the different regions of bone within the human MCs and MTs also provided evidence that these elements differ from one another. Higher canal numbers in the superior and inferior regions of the MCs as opposed to the MTs was found. Canal diameters also differed, being mainly larger in the MCs. In terms of cortical porosity, differences were also noted through analysis of resorption spaces. For example, in the medial and inferior regions of bone in the MTs, resorption was very high, whereas in the MCs, resorption spaces were numerous in the superior region.

Bar graphs (Figures 4.1 and 4.2) also indicate that human MCs and MTs differed from one another. The parameters Ca.V/TV, Ca.N and Ca.Narea of the MTs are greater

than those of the MCs. The 3D bar graph also indicates human MCs and MTs vary. Two out of the three parameters measured in 3D show higher results for the MTs.

5.1.3 Methodology

To test the validity of using Micro-CT as a methodology to investigate microscopic bone, ROIs from the 3D Micro-CT slices and the corresponding 2D histology sections were analyzed to see if it is possible to visually match them. Figure 4.5 shows a matched 2D and 3D ROI for both a bear and a human, indicating that matches were indeed possible and that the Micro-CT slices correspond quite well to the histology sections. It should be noted, however, that for some samples, matches were not as clear or were not possible.

Issues with matching the slices and sections are likely a result of specimen preparation. Histology sections produced to match the Micro-CT slices were manually cut on a low-speed diamond wafering saw (Buehler, Lake Bluff, USA) and manually ground on an automatic grinder (Buehler, Lake Bluff, USA). In using this type of thin-sectioning equipment, it is particularly difficult to align a bone completely straight in the low-speed saw and maintain even pressure when grinding down sections; therefore exact matches to the slices produced by Micro-CT were not achievable. However, the 2D measures used to statistically test against the 3D measures were directly derived from the Micro-CT slices through CTAn, thus 2D versus 3D analysis of the cortical bone structures measured for the human and bear sample set was not compromised. The ability to match the 2D sections and 3D slices has also been previously noted (Bagi et al., 2006; Cooper et al., 2004; Fajardo et al., 2002), thus promoting Micro-CT as a methodology to visualize and analyze 3D microscopic cortical bone.

Comparison of the 2D and 3D measures highlighted the benefits of analyzing bone in its 3D form. The measure of canal diameter indicates that in 2D, humans have larger canal diameters; yet in 3D the opposite is seen, bears display larger canal diameters. Hillier and Bell (2006: 257) note that in both human and nonhuman bone, an increase in canal numbers and canal diameters reflect an increase in remodeling and porosity. Bone remodeling is the mechanism that repairs and replaces damaged secondary bone, thus an increase in remodeling equates to an increase in secondary bone.

Histological analysis indicated that the bear bone was mainly secondary, whereas the human bone had a greater combination of primary and secondary bone. A possible explanation, then, of why bear canal diameters were higher than those of humans in 3D is that bears seem to have higher amounts of secondary bone. This indicates a potential increase in canal diameter which is recognized by Micro-CT as it is measuring entire canal volumes and thus providing a more representative measure of the canals, as opposed to the 2D measures which are simply taking a surface measure of the canal's diameters. This potential explanation also agrees with the 3D bar graph that indicates cortical porosity is higher in the bear bones. The way in which canal diameters were measured could also be a reason why the 2D and 3D measures differ. Bland-Altman data reveal that 2D measures underestimate canal diameter.

Another interesting comparison between the 2D and 3D data revealed differences in regards to canal numbers. Statistically, 3D measures indicated bears had significantly more canals than humans, which also agrees with the visual analysis of the histology sections and 3D bar graph. Interestingly, the 2D measures indicate the opposite, human canal populations are greater than bears. The Bland-Altman plot for canal number shows

that in 2D, canal numbers are overestimated, providing a possible explanation as to why discrepancies between human and bear canal populations are present.

5.1.4 Study limitations

At the start of this study, it was expected that statistically significant differences among and between the factors species and element would commonly be found; however, fewer than expected statistically significant findings were obtained. The small proportion of statistically significant results obtained is most likely a result of the main limitation of this study; small sample size.

Within-subjects analyses revealed no significant results between the paired cortical parameters for either humans or bears. While this finding was expected in the bears, as both their MCs and MTs are used for locomotion, the lack of significant difference between the human paired parameters was unexpected because humans do not use their MCs for locomotion. The issue of small sample size is most likely affecting this result. As previously discussed, r^2 values were calculated to identify variance between measures, and for human pairs 1, 2 and 5, medium to moderate effect sizes, 25.0, 25.0 and 49.0 respectively, were found. Such a finding may indicate that with a larger sample size these pairs may actually be statistically significant.

Averaged sample size calculations for each cortical parameter within the human sample set showed that an approximate sample size required to acquire potentially significance results is n=190. Generally, the required sample size for individual cortical parameters was quite small; 2D Ca.V/T.Ar (pair 1) (n=37), 3D Ca.V/TV (pair 2) (n=34), 3D Ca.N (pair 4) (n=61) and 2D Ca.Dm (pair 5) (n=13). That being said, 2D Ca.N (pair 3) and 3D Ca.Dm (pair 6) required much larger sample sizes, (n=804, 372) respectively.

Small sample size also proved to be problematic in regards to how data was analyzed. Initially, measurements for each cortical parameter were taken at the inferior, superior, lateral and medial aspect of each MC and MT because it was proposed that location within bone could reflect biomechanical loading as a result of mode of locomotion. However, due to small sample size, initial statistical testing was problematic as a lack of available degrees of freedom prohibited ROI analysis, thus all statistical analyses were carried out on the pooled ROI measures. This necessary aspect of analysis undoubtedly affected the results.

Small sample size also played a key role on how data was statistically analyzed overall. As previously discussed, deciding whether to use parametric or nonparametric tests are an important task, especially for small sample sizes. While the data for this research was found to be normally distributed, results such as these for small samples can potentially be problematic. Also, due to the nature of the specimens analyzed (i. e. human and bear bone) and where they were obtained (i. e. teaching collections and Manitoba Conservation) controlling for aspects such as population variance was difficult. Even with these inherent sample characteristics, a significant problem with nonparametric tests is that they essentially require larger sample sizes to obtain the same level of power to their parametric counterparts, and do not necessarily analyze all the information in a data set that is present. Therefore for this research, due to the normally distributed data, small sample sizes and interest in obtaining statistical power, parametric tests were chosen for analysis. Further investigation could however include running the nonparametric counterparts to these parametric analyses to further verify the validity of the results obtained.

Skedros et al. (2004) noted that cortical porosity measures differed depending on the region of bone analyzed. In subadult and adult specimens, cortical porosity increased in the caudal cortices by an average of 10.2% and 6.0%, respectively (Skedros et al., 2004: 288). Differences in cortical parameters as a result of the bone region they are measured in lends support to the argument that biomechanical forces exerted upon bone as a result of a species' mode of locomotion could in fact be evident within the microscopic structures of bone. Skedros et al. (2003) also noted that osteon shape tends to reflect the biomechanical forces exerted upon bone, and osteons of long bones are commonly circular in shape as they tend to parallel the direction of the major biomechanical force exerted.

If the human and bear ROIs measured for this study were able to be statistically compared to one another, potential differences and/or trends may be apparent due to the different mode of locomotion utilized by humans and bears and therefore varied biomechanical factors affecting different regions of bone. Histological analysis revealed bone microstructure did differ according to location within bone. As previously noted, resorption of the medial and inferior regions of bone in the MTs, was very high, whereas in the MCs, resorption was numerous in the superior region. It is not surprising that the resorption in the inferior region of MTs is high as this portion of the bone directly contacts the ground during locomotion.

Analysis of the different regions of bone from the histology sections revealed that microscopic cortical bone structure bone may in fact be a product of biomechanical loading. In the superior and inferior regions of both human and bear bone, osteons were typically round in shape, however in the medial and lateral regions, while round osteons

were present, elliptical shaped osteons were also prominent in both human and bear bone. Osteon densities also differed dependent upon the region of bone and element analyzed. Human MC superior and inferior bone regions showed higher amount of canals, whereas the medial and lateral regions of bone for both MCs and MTs displayed similar densities. In bears, all four bone regions for both MCs and MTs displayed similar osteon densities. Clearly, bone region and element have an affect on cortical bone structure supporting Skedros et al.'s (2003) aforementioned proposals.

The only cortical parameter that did not show any statistically significant results was cortical porosity. It should be noted that the Bland-Altman plot indicated that neither 2D or 3D were over nor underestimating the measure of cortical porosity, thus a methodological bias does not seem to be affecting cortical porosity measures. Cortical porosity reflects bone remodeling, which as previously noted is a bone's mechanism to respond and react to mechanical stimuli, thus differences between bears and humans were expected, but porosity is also a product of other mechanisms and a possible explanation for the lack of difference evident between the 2D and 3D measures leads to the another limitation; sample characteristics.

Age and cortical porosity are dependent factors, and studies have shown that as age increases, so too does the percentage of cortical porosity present within bone (Marie and Kassem, 2011; Cooper et al., 2004; Wachter et al., 2002; Parffit, 1984). The specific age of the human sample utilized in this study was not known, thus the age of each human MC/MT pair could only be estimated as adult based on the fully closed and obliterated lines of fusion at the epiphyses. If actual ages for the human sample were in proximity to one another, then by default a significant effect among the cortical porosity

measures would not necessarily be expected as cortical porosity measures would be relatively the same. This may be a reason why the within sample paired t-tests for the human sample set did not show significant results for the measure of cortical porosity.

The within paired t-tests for the bear sample also did not reveal statistically significant differences in cortical porosity, but, in the case of the bear sample set, age was available. Lack of significance could once again be a result of sample size although the possibility of black bears possessing a specialized bone regulatory mechanism due to their annual hibernation period could also be a potential explanation. Interestingly, Harvey and Donahue's (2004) study of black bear tibiae showed that increases in age did not result in an increase in cortical porosity. Due to the fact that black bears annually hibernate; experiencing a five to seven month period of bone disuse, Harvey and Donahue (2004: 1514) concluded that black bear bone has evolved to possess an "osteoregulatory mechanism." This osteoregulatory mechanism minimizes bone loss during hibernation through constant levels of osteoblastic formation and responds to any bone loss by increasing bone formation immediately after hibernation, termed "remobilization", thus age does not affect cortical porosity measures as typically seen in other mammals (Harvey and Donahue, 2004: 1514).

The relationship of age and cortical porosity in non-hibernating mammals showed the opposite of Harvey and Donahue's (2004) findings. Skedros et al. (2004) noted that mean cortical porosity measures in the calcanei of Rocky Mountain mule deer increased with age, particularly in subadult and adult age groups. If black bear bone does in fact feature an adaptive hibernation regulatory mechanism, it could potentially explain the lack of statistically significant difference displayed for cortical porosity among the bears

used in this particular study. It should be noted that Harvey and Donahue (2004) had a small sample size (n=16), and analyses could be conducted only at the end of the remobilization period due to conservation regulations.

Sample size calculations for the bear sample set within this study showed that an average of 40.2 individuals would be required for achieving potentially significant results. It would be of interest to run the same sample size calculations on Harvey and Donahue's (2004) data to reveal if larger sample sizes would also be required to further verify their findings regarding the relationship of cortical porosity and age. This would identify if their results are in fact a result of this proposed bone regulatory mechanism or if sample size was simply too small to detect a difference. Harvey and Donahue (2004) did not provide mean differences and standard deviations in their results, thus sample size estimates for their data could not be carried out.

Finally, methodology could also have affected the results. Analysis of cortical bone parameters such as canal size and porosity in 2D can be problematic due to the requirements of analysis. Microscopic bone structures such as osteons can inadvertently become altered through sample preparation requirements such as thin-sectioning. Jones et al. (2004: 126) noted 2D analysis based on the cylindrical geometry of osteons may be problematic. Longitudinally or obliquely transected canals as a result of processing may actually introduce bias and produce unreliable data by inaccurately omitting canals based on shape and geometric measures that are a product of sample preparation and not actual structural characteristics (Jones et al., 2004: 126). This could explain why some of the findings between the 2D measures and the visual analysis of the histology sections did not agree with one another. Potential sample preparation issues associated with 2D bone

analysis, further promotes the benefits of Micro-CT in that it analyzes bone within its natural 3D environment non-destructively and eliminates undesirable side effects of processing.

5.2 Conclusions

At the outset of this research it was hypothesized that biomechanically regulated microscopic cortical bone structures (i. e. cortical porosity, canal populations, canal diameter and polar moments of inertia) of the third metacarpals and metatarsals of both human hands/feet and black bear front/hind paws would reveal differences in the microscopic bone structures between their elements due to the fact that bears use their forelimbs for locomotion, whereas humans do not. It was also hypothesized that similarities in the microscopic bone structures between human feet and bear hind paws would be present because both species use these particular elements in a similar fashion, specifically for locomotion. Finally, comparison of two-dimensional and three-dimensional methodologies was performed to assess whether these microscopic morphologies can be accurately observed and analyzed non-destructively, through the use of microcomputed tomography imaging (Micro-CT). Results from this analysis, along with the striking similarity of the gross skeletal morphologies observed among bear and human third digits, were expected to provide support for the argument that comparative bone morphology, which is commonly used to define an individual's mode of locomotion, needs to be analyzed at the microscopic level.

Regions of bone analyzed by both Micro-CT and thin-sectioning could be visually matched, supporting the hypothesis that Micro-CT can in fact be utilized as a means to non-destructively analyze and accurately represent microscopic cortical bone structures

for both humans and bears in their natural 3D state. Furthermore, instances in this research found the Micro-CT data to coincide with the visual analysis of the histology sections, while agreement between the same parameter's 2D measures and histology sections was not always found, further highlighting the applicability of using Micro-CT as a means to analyze microscopic cortical bone. The possibility that a strictly two-dimensional analysis may inadvertently provide misleading data through damage of microscopic bone structures as a by-product of methodology, specifically thin-sectioning (Jones et al., 2004), could theoretically also be a factor within this research. As previously noted, canal numbers were found to be statistically, graphically and visually higher in bears, but 2D measures found humans to have higher canal numbers, which does not match the visual analysis of the histology sections. Without the added Micro-CT, bar graph and histology data, the result that humans have higher number of canals would be assumed, yet through data acquired from the bar graphs and histology sections, this finding for human canal populations may in fact not be accurate. This potential fault of 2D analysis again further promotes the benefit of utilizing 3D techniques such as Micro-CT for microscopic bone investigation.

Despite the small sample size of this study and the subsequent analysis issues as a result, 2D and 3D statistically significant results were still obtained, providing strong support that cortical bone structures do reflect differences in the MCs and MTs of humans and bears. Statistical results indicated in 3D that canal numbers significantly differ between human and bear MCs and MTs, and in 2D, canal diameters between human and bear MCs and MTs as well as MMI measures between human and bear MCs and MTs differed significantly.

High canal populations and large canal diameters are regarded as indicators of bone remodeling which in turn is an adaptive response to increased biomechanical loading, thus these results indicate that microscopic bone structures of bears and humans could be a reflection of the biomechanical forces exerted upon them due to mode of locomotion. An argument of this research is that microscopic bone morphology (as opposed to gross skeletal morphology) provides a more reliable method to infer species' modes of locomotion. Results from this study were inconclusive in regards to inferring species' modes of locomotion through microscopic cortical bone analysis, but as previously discussed small sample size was a key limitation. Differences between bear and human MCs and MTs at the microscopic level were observed, thus with a larger sample size, the argument that microscopic cortical bone structures can be used to infer a species mode of locomotion may potentially be supported.

Visual representation of the cortical structures assessed through bar graphs and histology sections identified trends between the bear and human MCs and MTs that were not always statistically recognized. Within-subjects paired t-tests did not reveal significant differences among the MCs and MTs of humans Visual analysis of the regions of interest in the histology sections revealed that differences between elements in the human sample may actually be present. For example, canal numbers were more numerous in the superior and inferior regions of the MCs and canal diameters were found to be larger in the MCs. Especially because differences among the MCs and MTs of the human sample were noted within different regions of bone, a larger sample size that would warrant statistical analysis of the ROIs could indicate that the MCs and MTs among the humans significantly vary as a result of locomotion.

As a measure of validity, observation of the histology sections for the bear sample agreed with the paired t-test results, in that differences between the MCs and MTs should not significantly differ because bears use both their forelimbs and hindlimbs for locomotion. Canal numbers were high in both the MCs and MTs among the bears. Canal diameters also were similar in size between the MCs and MTs. From the agreement between the bear paired t-tests and histology sections, it then seems justifiable that even though they are not statistically significant, differences between the microscopic cortical structures of the human MCs and MTs potentially lend support to the hypothesis that these elements vary because humans do not use their forelimbs for locomotion.

In terms of differences between elements, variation between the MCs of the bears and humans are displayed. Large canal diameters are noted as indicators of increased remodeling and porosity (Hillier and Bell, 2006). This finding lends support to the hypothesis that differences between the MCs of humans and bears would be present due to the fact that bears use their forelimbs for locomotion whereas humans do not, thus the biomechanical forces exerted as a result of this factor are evident within the microscopic bone structures.

From this result, it could be assumed that the MCs of bears would be more porous and that porosity between the MTs of the humans and bears would be similar. Both the 2D and 3D bar graphs support this assumption. Visual representations of the statistics and the histology sections further support the hypothesis that bear and human MCs and MTs differ from one another as a result of mode of locomotion, and microscopic cortical bone structures can be used as biomechanical indicators to infer species modes of locomotion.

In conclusion, the statistical, graphical and visual results of this research provide strong evidence that the microscopic cortical bone structures between human and black bear metacarpals and metatarsals differ from one another, which could potentially be a reflection of their different modes of locomotion. Cortical porosity, canal populations, canal areas/volumes and polar moments of inertia were all proposed as useful indicators of the biomechanical forces exerted upon bone. Bone remodeling is not always a result of mechanical loading, yet the cortical microstructures analyzed did differ among the superior, inferior, medial and lateral ROIs, supporting the application of these bone microstructures as biomechanical indicators for this research.

Micro-CT was proposed as a novel 3D methodology to non-destructively analyze microscopic cortical bone within its natural three-dimensional state, thus providing a more comprehensive and accurate assessment of the three-dimensional property of bone. Visually matched bone regions of interest between the two-dimensional thin sections and three-dimensional Micro-CT slices, as well as comparison of the Micro-CT data to the statistic results and bar graphs, indicate that Micro-CT can in fact be utilized as a valid means to non-destructively analyze the microscopic structures of cortical bone. As previously stated, one of the most significant features of micro-CT is that it is a completely non-invasive tool that can be used for analyzing the microscopic characteristics of sensitive materials such as human and ancient fossil remains. The types of data that were obtained non-destructively in this research shows that three-dimensional methodologies such as Micro-CT would be an invaluable tool for evolutionary researchers who attempt to define the locomotor repertoires of ancient hominins.

In regards to inferring ancient hominin species' modes of locomotion, comparison of the remarkably similar skeletal elements between human hands/feet and bear front/hindlimbs, revealed that they do in fact differ from one another microscopically, a result that is not indicated at the gross morphology level. Differentiation of a species mode of locomotion using microscopic cortical bone structures was not found, but as previously explained, with larger sample sizes differentiation may be possible. Due to the non-destructive nature of Micro-CT, comprehensive and informative analysis of the microscopic characteristics of ancient hominin bone, if available, may in fact provide a more accurate representation of their respective modes of locomotion. Microscopic bone analysis could also potentially be used as a means of species identification because cortical bone structures can be utilized to differentiate between species (Hillier and Bell, 2006). Three-dimensional technology such as Micro-CT that has the capability to non-invasively analyze microscopic bone in its natural 3D state would prove as an invaluable resource for evolutionary anthropologists.

Finally, while two-dimensional measures such as polar moment of inertia are useful indicators of bone geometric parameters as evidenced in this research, microscopic analyses of cortical bone provide an invaluable 3D compliment to traditional bone analysis techniques which are not possible through a strictly gross skeletal morphology analysis.

Overall, even with the small sample size, this research has provided evidence that human and black bear metacarpals and metatarsals do vary and microscopic cortical bone structures, specifically cortical porosity, canal populations, canal diameter and polar moments of inertia can serve as indicators of biomechanical loading. Although the

results of this study did not differentiate mode of locomotion, histological analysis of the human MCs and MTs did reveal differences between them. Sample size was a key limitation for this research and with larger sample sizes, the hypothesis that microscopic cortical bone structures can be used to differentiate a species mode of locomotion may be supported. The results from this initial study indicate that this is an area of research that merits further investigation.

5.3 Suggestions for Further Research

As commonly found with research, unexpected results provoke more questions and ideas not initially recognized or addressed. From this research, the following suggestions for further investigation are recommended:

1) Most notably, a larger sample size is recommended so more advanced statistical analyses can be carried out, potentially revealing significant results of the trends noted via the graphical and visual analyses. Control over other variables such as the age and sex of the sample would also aid in removing potential bias from factors such as these.

2) While not as strikingly similar as the elements that comprise human hands and feet and black bear front/hind paws, the long bones of humans and black bears, such as the femur and humerus are also remarkably similar to one another. Similar procedures and methods used in this research could be carried out on the long bones of humans and black bears to see if results compare to those of this research.

3) The results of this research could also be taken in a completely different direction by comparing the microscopic cortical bone parameters from a forensic standpoint. Cortical bone structures such as Haversian system area and canal diameter have been proposed as useful indicators to differentiate between human and nonhuman bone. Osteon banding

patterns has also been noted as typical of nonhuman bone, however due to the presence of osteon banding in one of the human samples, when only five individual humans were analyzed of which only two were histologically investigated, further investigation into this identification characteristic is warranted.

REFERENCES CITED

Altman, D. G. and J. M. Bland
1983 Measurement in Medicine: The Analysis of Method Comparison Studies. *Journal of the Royal Statistical Society. Series D (The Statistician)* 307-317.

Augat, P. H. Reeb and L. E. Claes
1996 Predictions of fracture load at different skeletal sites by geometric properties of the cortical shell. *Journal of Bone and Mineral Research* 11: 1356-1363.

Bartley, M. H., J. S. Arnold, R. K. Haslam and W. S. S. Jee
1966 The relationship of bone strength and bone quality in health, disease and aging. *Journal of Gerontology* 21: 517-521.

Basillais, A., S. Bensamoun, C. Chappard, B. Brunet-Imbault, G. Lemineur, B. Ilharreborde, M-C. Ho Ba Tho and C-L Benhamou
2007 Three-dimensional characterization of cortical bone microstructure by microcomputed tomography: validation with ultrasonic and microscopic measurements. *Journal of Orthopaedic Science* 12: 141-148.

Berillon, G.
2003 Assessing the Longitudinal Structure of the Early Hominid Foot: A Two-dimensional Architecture Analysis. *Human Evolution* 18: 113-122.

Biewener, A. A.
1991 Musculoskeletal design in relation to body size. *Journal of Biomechanics* 24(1): 19-29.

Borah, B., G. J. Gross, T. E. Dufresne, T. S. Smith, M. D. Cockman, P. A. Chmielewski, M. W. Lundy, J. R. Hartke and E. W. Sod
2001 Three-Dimensional Microimaging (MRμI and μCT), Finite Element Modeling, and Rapid Prototyping Provide Unique Insights Into Bone Architecture in Osteoporosis. *The Anatomical Record (New Anat.)* 265: 101-110.

Bouxsein, M. L., S. K. Boyd, B. A. Christiansen, R. E. Guldberg, K. J. Jepsen and R. Müller
2010 Guidelines for Assessment of Bone Microstructure in Rodents Using Micro-Computed Tomography. *Journal of Bone and Mineral Research* 25(7): 1468-1486.

Burr, D. B., A. G. Robling and C. H. Turner
2002 Effects of Biomechanical Stress on Bones in Animals. *Bone* 30(5): 781-786.

Byers, N. S.
2008 *Introduction to Forensic Anthropology: A Textbook.* 3rd ed. Allyn and Bacon, Boston.

Carter, D. R., C. H. van der Muelen and G. S. Beaupré
1996 *Skeletal development: mechanical consequences of growth, aging and disease.* In R. Marcus, D. Feldman and J. Kelsey, editors. Osteoporosis. Academic Press, San Diego, California: 333-348.

CBC News
2009 World – 'Foot' found in trash turns out to be a bear paw. Electronic document, http://www.cbc.ca/news/world/story/2009/08/07/-foot-garbage-bear-paw.html

Chen, Y-S., C. Ramachandra and S. N. Tewari
2004 Structural differences in the cortical bone of Turkey tibia. *Journal of Material Science* 39: 207-214.

Clark, R. J. and P. V. Tobias
1995 Sterkfontein member 2 foot bones of the oldest South African hominid. *Science* 269: 521-524.

Cole, J. H. and M. C. H. van der Muelen
2011 Whole Bone Mechanics and Bone Quality. *Clinical Orthopaedics and Related Research* 469: 2139-2149.

Cooper, D. M. L., B. Erickson, A. G. Peele, K. Hannah, C. D. L. Thomas and J. G. Clement
2011 Visualization of 3D osteon morphology by synchrotron radiation micro-CT. *Journal of Anatomy* 219: 481-489.

Cooper, D., A. Turinsky, C. Sensen and B. Hallgrimsson
2007 Effect of Voxel Size on 3D Micro-CT Analysis of Cortical Bone Porosity. *Calcified Tissue International* 80: 211-219.

2003 Quantitative 3D Analysis of the Canal Network in Cortical Bone by Micro-Computed Tomography. *The Anatomical Record (Part B: New Anat.)* 247B: 169-179.

Cooper, D. M. L., C. D. L. Thomas, J. G. Clement and B. Hallgrimsson
2006 Three-Dimensional Microcomputed Tomography Imaging of Basic Multicellular Unit-Related Resorption Spaces in Human Cortical Bone. *The Anatomical Record Part A* 288A: 806-816.

Cooper, D. M. L., J. R. Matyas, M. A. Katzenberg and B. Hallgrimsson
2004 Comparison of Microcomputed Tomographic and Microradiographic Measurements of Cortical Bone Porosity. *Calcified Tissue International* 74: 437-447.

Currey, J.

1984 *The Mechanical Adaptations of Bones.* Princeton University Press, Princeton, New Jersey.

Enlow, D. H.
1975 Handbook of facial growth. W. B. Saunders, Philadelphia.

Enlow, D. H.
1963 *Principles of Bone Remodelling*. Charles C Thomas, Springfield, Illinois.

Fajardo, R. J., T. M. Ryan and J. Kappelman
2002 Assessing the Accuracy of High-Resolution X-Ray Computed Tomography of Primate Trabecular Bone by Comparisons with Histological Sections. *American Journal of Physical Anthropology* 118: 1-19.

Feldkamp, L. A., S. A. Goldstein, A. M. Parfitt, G, Jesion and M. Kleerekoper
1989 The direct examination of three-dimensional bone architecture in vitro by computed tomography. *Journal of Bone and Mineral Research* 4: 3-11.

Foote, J. S.
1916 A Contribution to the Comparative Histology of the Femur. *Smithsonian Contributions to Knowledge* 35(3).

Frost, M. Harold
1969 Tetracycline-based Histological Analysis of Bone Remodeling. *Calcified Tissue Research* 3: 211-237.

Gross, T. S., K. J. McLeod and C. T. Rubin
1992 Characterizing bone strain distributions in vivo using three triple rosette strain gages. *Journal of Biomechanics* 25: 1081-1087.

Hanson, N. A. and C. M. Bagi
2004 Alternative approach to assessment of bone quality using micro-computed tomography. *Bone* 35: 326-333.

Harcourt-Smith, W. E. H. and L. C. Aiello
2004 Fossils, feet and the evolution of human bipedal locomotion. *Journal of Anatomy* 204(5): 403-416.

Hassard, T. H.
1991 *Understanding Biostatistics*. Mosby – Year Book, Inc. St. Louis, Missouri.

Hebblewhite, M., M. Percy and R. Serrouya
2003 Black bear (Ursus americanus) survival and demography in the Bow Valley of Banff National Park, Alberta. *Biological Conservation* 112: 415-425.

Hillier, M. L. and L. S. Bell

2007 Differentiating Human Bone from Animal Bone: A Review of Histological Methods. *Journal of Forensic Science* 52(2): 249-263.

Hoyte, D. A. N. and D. H. Enlow
1966 Wollf's law and the problem of muscle attachment on resorptive surfaces of bone. *American Journal of Physical Anthropology* 24: 205-214.

Jaworski, Z. F. G.
1976 *Three dimensional view of the gross and microscopic structures of adult human bone.* In Jaworski Z. F. G., editor. Proceedings of the first workshop on bone morphometry; March 28-1, 1973, Ottawa, Canada. Ottawa, Canada: University of Ottawa Press, 1976: 3-7.

Jones, A. C., A. P. Sheppard, R. M. Sok, C. H. Arns, A. Limaye, H. Averdunk, A. Brandwood, A. Sakellariou, T. J. Senden, B. K. Milthorpe and M. A. Knackstedlt
2004 Three-dimensional analysis of cortical bone structure using X-ray micro-computed tomography. *Physica A: Statistical Mechanics and its Applications* 339: 125-130.

Junger, W. L.
1982 Lucy's limbs: Skeletal allometry and locomotion in Australopithecus afarensis (A. L. 288-1). *Nature* 297: 676-678.

Jungers, W. L. and R. J. Minns
1979 Computed Tomography and Biomechanical Analysis of Fossil Long Bones. *American Journal of Physical Anthropology* 50: 265-290.

Komar, D. A. and J. E. Buikstra
2008 *Forensic Anthropology: Contemporary Theory and Practice.* Oxford University Press, New York.

Kontulainen, S., D. Liu, S. Manske, M. Jamieson, H. Sievänen and H. McKay
2007 Analyzing Cortical Bone Cross-Sectional Geometry by Peripheral QCT: Comparison With Bone Histomorphometry. *Journal of Clinical Densitometry* 10(1): 86-92.

Kuhn, J. L., S. A. Goldstein, L. A. Feldkamp, R. W. Goulet and G. Jesion
1990 Evaluation of a microcomputed tomography system to study trabecular bone structure. *Journal of Orthopaedic Research* 8: 833-842.

Latimer, B. and O. C. Lovejoy
1990 Hallucial tarsometatarsal joint in Australopithecus afarensis. *American Journal of Physical Anthropology* 82: 125-133.

Lanyon, L. E.
1984 Functional Strain as a Determinant for Bone Remodeling. *Calcified Tissue*

International 36: 56-61.

Lanyon, L. E., W. G. Hampson, A. E. Goodship and J. S. Shah
1975 Bone deformation recorded in vivo from strain gauges attached to the human tibial shaft. *Acta Orthopaedica* 46: 256-268.

Lanyon, L. E. and D. G. Baggott
1976 Mechanical function as an influence of the structure and form of bone. *The Journal of Bone and Joint Surgery British* 58B: 436-443.

Lovejoy, O. C., B. Latimer, G. Suwa, B. Asfaw and T. D. White
2009 Combining Prehension and Propulsion: The Foot of *Ardipithecus ramidus*. *Science* 326: 72e1-72e7.

Marchi, Damiano
2005 The cross-sectional geometry of the hand and foot bones of the Hominoidea and its relationship to locomotor behavior. *Journal of Human Evolution* 49: 743-761.

Merz, W. A. and R. K. Schenk
1970 Quantitative structural analysis of human cancellous bone. *Acta Anatomica* 75: 54-66.

Motulsky, M.
2010 *Intuitive Biostatistics A Nonmathematical Guide to Statistical Thinking*. 2nd ed. Oxford University Press, New York.

Mulhern, D. M. and D. H. Ubelaker
2001 Differences in Osteon Banding between Human and Nonhuman Bone. *Journal of Forensic Science* 46(2): 220-222.

Müller, Ralph
2009 Hierarchical microimaging of bone structure and function. *Nature Reviews Rheumatology* 5: 373-381.

Nordin, M. and V. H. Frankel
2001 *Basic Biomechanics of the Musculoskeletal System.* 3rd ed. Lippincott Williams & Wilkens, Baltimore, Maryland.

Parfitt, A. M.
2002 Targeted and Nontargeted Bone Remodeling: Relationship to Basic Multicellular Unit Organization and Progression. *Bone* Vol. 30(1): 5-7.

Parfitt, M. A., M. K. Drezner, F. H. Glorieux, J. A. Kanis, H. Malluche, P. J. Meunier, S. M. Ott and R. R. Recker
1987 Bone Histomorphometry: Standardization of Nomenclature, Symbols, and Units: Report of the ASBMR Histomorphometry Nomenclature Committee. *Journal of*

Bone and Mineral Research 2(6): 595-609.

Parfitt, M. A., C. H. E. Mathews, A. R. Villanueva, M. Kleerekoper, B. Frame, D. S. Rao
1983 Relationships between surface, volume, and thickness of iliac trabecular bone in aging and osteoporosis. *Journal of Clinical Investigation* 72: 1396-1409.

Petrtýl, M., J. Heft and P. Fiala
1996 Spatial Organization of the Haversian Bone in Man. *Journal of Biomechanics* 29(2): 161-169.

Radin, E. L., H. G. Parker, J. W. Pugh, R. S. Steingberg, I. L. Paul and R. M. Rose
1973 Response of joint to impact loading-III: Relationship between trabecular microfractures and cartilage degeneration. *Journal of Biomechanics* 6: 51-57.

Rüegsegger, R., B. Koller and R. Müller
1995 A Microtomographic System for the Nondestructive Evaluation of Bone Architecture. *Calcified Tissue International* 58: 24-29.

Seeman, Ego
2008 Bone quality: the material and structural basis of bone strength. *Journal of Bone Mineral Metabolism* 26: 1-8.

Seeman, E. and P. D. Delmas
2006 Bone Quality – The Material and Structural Basis of Bone Strength and Fragility. *The New England Journal of Medicine* 354: 2250-2261.

Simon, S. R. and E. L. Radin
1972 The response of joints to impact loading-II. In vivo behaviour of subchondral bone. *Journal of Biomechanics* 5: 267-272.

Sims, M. E.
2007 *Comparison of Black Bear Paws to Human Hands and Feet*. Identification Guides for Wildlife Law Enforcement No. 11. USFWS, National Fish and Wildlife Forensics Laboratory, Ashland, Oregon.

Skedros, J. G., K. J. Hunt and R. D. Bloebaum
2004 Relationships of Loading History and Structural and Material Characteristics of Bone: Development of the Mule Deer Calcaneus. *Journal of Morphology* 259: 281-307.

Skedros, J. G., C. L. Sybrowsky, T. R. Parry and R. D. Bloebaum
2003 Regional Differences in Cortical Bone Organization and Microdamage Prevalence in Rocky Mountain Mule Deer. *The Anatomical Record Part A* 247A: 837-850.

Sommerfeldt, D. W. and C. T. Rubin

2001 Biology of bone and how it orchestrates the form and function of the skeleton. *European Spine Journal* 10: 86-95.

Steele, D. G. and C. A. Bramblett
2003 *The Anatomy and Biology of the Human Skeleton.* 7th ed. Texas A&M University Press, College Station, Texas.

Stewart, T. D.
1959 Bear Paw Remains Closely Resemble Human Bone. *FBI Law Enforcement Bulletin* 28(1): 18-21.

Stout, S. D.
2003 *Small bones of contention*. In: Steadmen DW, editor. Hard evidence: cases studies in forensic anthropology. Prentice Hall, Upper Saddle River, New Jersey, 234-244.

Stout, S. D., B. S. Brunsden, C. F. Hildebolt, P. K. Commean, K. E. Smith and N. C. Tappen
1999 Computer-Assisted 3D Reconstruction of Serial Sections of Cortical Bone to Determine the 3D Structure of Osteons. *Calcified Tissue International* 65: 280-284.

Turner, C. H.
1998 Three Rules for Bone Adaptation to Mechanical Stimuli. *Bone* 23(5): 399-407.

Wachter, N. J., G. D. Krischak, M. Mentzel, M. R. Sarkar, T. Ebinger and L. Kinzl
2002 Correlation of Bone Mineral Density With Strength and Microstructural Parameters of Cortical Bone In Vitro. *Bone* 31(1): 90-95.

Walker, A.
1973 New *Australopithecus* femora from East Rudolf, Kenya. *Journal of Human Evolution* 6(2): 545-555.

White, T. D. and P. A. Folkens
2005 *The Human Bone Manual*. Elsevier Academic Press, San Diego, California.

Wolff, J.
1892 *Das Gesetz der Transformation der Knochen.* Hirschwald, Berlin.

APPENDIX A: MANITOBA CONSERVATION PERMIT

Manitoba Conservation

WB08992
Valid Manitoba Conservation

Dead Wild Animal Possession Permit

Subject to the provisions of *The Wildlife Act*, the regulations made thereunder and the conditions set out in this permit:

Permit Holder:	Brandon University Dept. of Anthropology 270 – 18th Street Brandon MB R7A 6A9 Att'n: Suyoko Tsukamoto

Is hereby authorized to possess the following dead wild animal(s) or parts thereof for educational purposes:

Species:	Wild Animals as listed in Schedule A of The Wildlife Act.

At, within or on the following location:

Location:	270 – 18th Street, Brandon MB

Conditions:

1	Wild animal specimens or parts thereof that are authorized to be kept under authority of this permit may not be sold, permanently transferred or given to another person or institution without prior written authorization from the Director, Wildlife and Ecosystem Protection Branch.
2	The authority granted by this permit is limited to (i) an employee or subcontractor of the permit holder while engaged in duties approved or required by the permit holder, or (ii) an associate, or a person supervising or working under the supervision of the permit holder. The permit holder shall provide such person, when in possession of a specimen away from the authorized location, with a counter-signed and dated photocopy of this permit.
3	The permit holder may accept specimens directly from the public with authority to keep any specimen so received subject to the approval of the Director, Wildlife and Ecosystem Protection Branch.
4	The permit holder shall maintain on the authorized location an up to date written inventory of all specimens authorized under this permit. The inventory shall list the name of the species, quantity, description of item or part if it is not a whole animal, status or preservation method, e.g., frozen, dried, full-body mount, tanned, study skin, other form of preservation (describe) and origin and, if destroyed or deleted from inventory, the reason.
5	The permit holder will submit to the Director of Wildlife and Ecosystem Protection an inventory that lists the name of the species, quantity, description of item or part if it is not a whole animal, status or preservation method, e.g., frozen, dried, full-body mount, tanned, study skin, other form of preservation (describe) and origin that were added to the collection and, if destroyed or deleted from inventory, the reason.
6	The Government of Manitoba shall not be held responsible or liable for any damage, injury or loss sustained to the person or property of the permit holder or for any damage, injury or loss sustained by any other person or the property of any other person as a result of the exercise of a right or privilege granted herein.
7	This permit may be cancelled or the conditions amended at any time.
8	The permit holder shall make written application for permit renewal on or before expiry date of this permit.
9	The exercise, by the permit holder, of a right or privilege granted herein shall be construed as acceptance of and agreement to comply with the conditions set out herein.

Date Issued: December 22, 2008	**Issued By:**
Expiry Date: March 31, 2014	**For Minister of Conservation**

FORM REVISED: MARCH 2005

Excerpts from *The Wildlife Act*

A permit and the rights and privileges granted thereunder are not transferable to another person.

A permit must be carried while exercising a right or privilege granted thereunder or kept on the premises where a specimen is being held and be produced upon the request of an officer.

In addition to any other permit that may be held, an import or export permit must be obtained before bringing a wild animal or part thereof into Manitoba or taking or shipping a wild animal or part thereof out of Manitoba.

APPENDIX B: TABLES

TABLE 4.1 One sample Kolomogorov-Smirnov Test for Average 2D Cortical Parameters

		Ca.V/TV-MC	Ca.V/TV-MT	Ca.N-MC	Ca.N-MT	Ca.Dm-MC	Ca.Dm-MT	MMI-MC	MMI-MT
N		10	10	10	10	10	10	10	10
Normal Parameters[a b]	Mean	9.9883	10.0717	12.5875	11.93	.0155	.0187	534.2074500	484.0738230
	Std. Deviation	5.46895	4.97561	10.43084	7.38862	.00960	.01280	306.63846265	284.56773031
Most Extreme Differences	Absolute	.151	.186	.349	.170	.215	.156	.244	.218
	Positive	.151	.186	.349	.170	.215	.156	.244	.218
	Negative	-.122	-.149	-.225	-.155	-.142	-.126	-.159	-.156
Kolmogorov-Smirnov Z		.478	.587	1.104	.538	.681	.492	.773	.688
Asymp. Sig. (2-tailed)		.976	.881	.175	.934	.742	.969	.589	.731

a. Test distribution is normal
b. Calculated from data

Abbreviations: Ca.V/TV (cortical porosity); Ca.N (canal number); Ca.Dm (canal diameter); MMI (polar moment of inertia); MC (metacarpal); MT (metatarsal).

TABLE 4.2 One sample Kolmogorov-Smirnov Test for Average 3D Cortical Structures

		Ca.V/TV-MC	Ca.V/TV-MT	Ca.N-MC	Ca.N-MT	Ca.Dm-MC	Ca.Dm-MT
N		10	10	10	10	10	10
Normal Parameters[a b]	Mean	9.5158	9.2600	7.3473	7.6875	71.2325	62.1800
	Std.	5.27476	4.33530	3.04817	3.90718	58.15271	35.66175
Most Extreme Differences	Absolute	.140	.151	.144	.193	.285	.229
	Positive	.140	.151	.136	.193	.285	.229
	Negative	-.118	-.100	-.144	-.130	-.196	-.183
Kolmogorov-Smirnov Z		.443	.479	.454	.612	.902	.725
Asymp. Sig. (2-tailed)		.989	.976	.986	.849	.390	.689

a. Test distribution is normal
b. Calculated from data

Abbreviations: Ca.V/TV (cortical porosity); Ca.N (canal number); Ca.Dm (canal diameter); MMI (polar moment of inertia); MC (metacarpal); MT (metatarsal).

TABLE 4.4 Independent T-test average ROI results for the stratified sample

Parameter	Levene's Test for Equality of Variance		t-test for Equality of Means				95% Confidence Interval of the Difference		r2
	F	Sig	t	Sig. (2-tailed)	Mean Difference	Std. Error Diff	Lower	Upper	
Ca.V/TV									
2D MC	1.820	.214	1.779	.113	5.52558	3.10527	-1.63519	12.68635	28.3
2D MT	.035	.856	.175	.856	.58379	3.33135	-7.09833	8.26591	0.4
3D MC	1.953	.200	1.635	.141	5.00832	3.06349	-2.05610	12.07274	25.0
3D MT	.071	.797	-.278	.788	-.80602	2.89421	-7.48008	5.86804	0.1
Ca.N									
2D MC	.192	.673	-.239	.817	-1.665500	6.97241	-17.74341	14.41341	0.71
2D MT	1.361	.277	-1.085	.310	-5.02000	4.62776	-15.69164	5.65164	12.8
3D MC	1.586	.243	3.862	.005*	4.66600	1.20816	1.87997	7.45203	65.1
3D MT	2.970	.123	5.325	.001*	6.54710	1.22949	3.71189	9.38231	78.0
Ca.Dm									
2D MC	1.466	.261	-.223	.829	-1.43	.6.42	-16.42	13.38	0.6
2D MT	.123	.735	-2.716	.026*	-15.88	.5.85	-29.36	-2.40	48.0
3D MC	2.760	.135	.887	.401	33.00500	37.22386	-52.83337	118.84337	9.0
3D MT	7.148	.028	.075	.942	1.79000	23.91426	-53.35638	56.93638	0.1
MMI									
2D MC	10.086	.013	4.938	.001*	508.138500	102.909539	270.828675	745.448324	84.8
2D MT	4.189	.075	7.118	.000*	501.767926	70.4916694	339.213844	664.322007	90.8

Abbreviations: Ca.V/TV (cortical porosity); Ca.N (canal number); Ca.Dm (canal diameter); MMI (polar moment of inertia); MC (metacarpal); MT (metatarsal); AVG (average).
*$p < 0.05$